RESEARCH ARTICLE

Functional membrane microdomains and the hydroxamate siderophore transporter ATPase FhuC govern Isd-dependent heme acquisition in *Staphylococcus aureus*

Lea Antje Adolf[1,2,3], Angelika Müller-Jochim[1,2,3], Lara Kricks[4,5,6], Jan-Samuel Puls[7], Daniel Lopez[4,5,6], Fabian Grein[7,8], Simon Heilbronner[1,2,3,9,10]*

[1]Department of Infection Biology, Interfaculty Institute of Microbiology and Infection Medicine, University of Tübingen, Tübingen, Germany; [2]Cluster of Excellence EXC 2124 Controlling Microbes to Fight Infections, Tübingen, Germany; [3]Interfaculty Institute of Microbiology and Infection Medicine, Institute for Medical Microbiology and Hygiene, UKT Tübingen, Tübingen, Germany; [4]National Centre for Biotechnology, Spanish National Research Council (CNB-CSIC), Madrid, Spain; [5]Research Centre for Infectious Diseases (ZINF), University of Würzburg, Würzburg, Germany; [6]Institute for Molecular Infection Biology (IMIB), University of Würzburg, Würzburg, Germany; [7]Institute for Pharmaceutical Microbiology, University Hospital Bonn, University of Bonn, Bonn, Germany; [8]German Center for Infection Research (DZIF), partner site Bonn-Cologne, Bonn, Germany; [9]German Center for Infection Research (DZIF), Tübingen, Germany; [10]Faculty of Biology: Microbiology, Ludwig-Maximilians-Universität München, München, Germany

***For correspondence:** simon.heilbronner@bio.lmu.de

Competing interest: The authors declare that no competing interests exist.

Funding: See page 18

Received: 01 December 2022
Preprinted: 13 January 2023
Accepted: 11 April 2023
Published: 12 April 2023

Reviewing Editor: Bavesh D Kana, University of the Witwatersrand, South Africa

Abstract Sufficient access to transition metals such as iron is essential for bacterial proliferation and their active limitation within host tissues effectively restricts infection. To overcome iron limitation, the invasive pathogen *Staphylococcus aureus* uses the iron-regulated surface determinant (Isd) system to acquire hemoglobin-derived heme. While heme transport over the cell wall is well understood, its transport over the membrane is hardly investigated. In this study, we show the heme-specific permease IsdF to be energized by the general ATPase FhuC. Additionally, we show that IsdF needs appropriate location within the membrane for functionality. The membrane of *S. aureus* possesses special compartments (functional membrane microdomains [FMMs]) to organize membrane complexes. We show IsdF to be associated with FMMs, to directly interact with the FMM scaffolding protein flotillin A (FloA) and to co-localize with the latter on intact bacterial cells. Additionally, Isd-dependent bacterial growth required FMMs and FloA. Our study shows that Isd-dependent heme acquisition requires a highly structured cell envelope to allow coordinated transport over the cell wall and membrane and it gives the first example of a bacterial nutrient acquisition system that depends on FMMs.

Editor's evaluation

In this fundamental manuscript, the authors provide compelling evidence that a housekeeping ATPase is required for heme utilization in the important pathogen *Staphylococcus aureus* through its interaction with the canonical heme transporter in this organism. The authors convincingly show that this complex associates with functional membrane microdomains and thus establishes a new paradigm for regional localization of the heme transport system in the staphylococci.

The work will be of interest to microbiologists, particularly those studying transport for macromolecules.

Introduction

Transition metals such as iron, manganese, copper, and zinc are essential trace elements for all kingdoms of life. Due to their redox potential, transition metals can convert between divalent and trivalent states making them ideal to support enzymatic processes. Molecular iron is of major importance in this regard as it is essential for several central metabolic and cellular processes including glycolysis, oxidative decarboxylation, respiration, and DNA replication (**Schaible and Kaufmann, 2004**). Accordingly, appropriate acquisition of iron is essential for bacterial growth and this dependency is a major target for eukaryotic innate immune strategies to limit bacterial infections. Targeted depletion of human body fluids from trace metals effectively limits bacterial proliferation and is referred to as nutritional immunity (**Murdoch and Skaar, 2022**; **Weinberg, 1975**). To overcome host-induced iron starvation, bacterial pathogens have developed a range of strategies to acquire iron during infection (**Sheldon et al., 2016**). They can secrete siderophores, which possess sufficient affinity toward Fe^{3+} to extract the ion from host-chelating molecules (e.g. transferrin, lactoferrin) (**Miethke and Marahiel, 2007**). *Staphylococcus aureus* secretes the carboxylate-type siderophores staphyloferrin A (SA) and staphyloferrin B (SB), and their iron-saturated forms are acquired by the membrane-located HtsABC and SirABC systems, respectively (**Beasley et al., 2009**; **Cheung et al., 2009**). Additionally, *S. aureus* expresses systems for acquisition of siderophores produced by other bacterial species (xenosiderophores). The $FhuBGCD_1D_2$ system enables acquisition of hydroxamate-type siderophores (**Sebulsky and Heinrichs, 2001**) and the SstABCD system allows acquisition of iron-chelating molecules of the catecholate-type including xenosiderophores, but also human-derived catecholamine stress hormones like epinephrine, norepinephrine, or dopamine (**Beasley et al., 2011**). Moreover, the FeoAB transporter presumably allows acquisition of inorganic Fe^{2+}(**Sheldon and Heinrichs, 2015**). In humans, much of the iron is bound to heme in hemoglobin (Hb), which can be released from erythrocytes by the action of cytolytic toxins (**Cassat and Skaar, 2013**; **Spaan et al., 2015**). A well-known mechanism for heme acquisition is the iron-regulated surface determinant (Isd) systems. This was first described for the invasive pathogen *S. aureus* (**Mazmanian et al., 2003**). Similar systems have since been identified in *Staphylococcus lugdunensis* (**Heilbronner et al., 2016**), *Staphylococcus capitis*, and *Staphylococcus caprea* (**Sun et al., 2020**) as well as in phylogenetically more distant Gram-positive pathogens such as *Bacillus anthracis* (**Gat et al., 2008**; **Maresso et al., 2006**), *Bacillus cereus* (**Abi-Khalil et al., 2015**), and *Listeria monocytogenes* (**Klebba et al., 2012**; **Xiao et al., 2011**). All Isd systems contain surface-anchored molecules to extract heme from host hemoproteins and to guide it over the cell wall to a membrane-located ATP-binding cassette (ABC) transporter. In the cytosol, the heme is degraded to release ionic iron. The Isd system of *S. aureus* is best studied (**Sheldon and Heinrichs, 2015**). Here, the cell wall-anchored proteins (CWAs) IsdB and IsdH bind Hb and Hb-haptoglobin complexes, respectively. Heme is removed from the hemoproteins by IsdA and IsdB and transferred to IsdC in the cell wall. Heme is then transferred to the heme-specific lipoprotein IsdE on the outer leaflet of the cell membrane. The permease IsdF functions as homodimer and transports heme into the cytosol. There, the two monooxygenases IsdG and IsdI release iron from heme.

The passage of heme across the cell wall of *S. aureus* has been studied in great detail. In contrast, the process of heme transport across the membrane remains somewhat undefined. Importantly, an ATPase is not encoded within the *isd* operon of *S. aureus*, raising the question of how the transport of heme is energized. Additionally, it is unclear if heme funneling across the cell wall demands the membrane transporter to be in a specific location within the liquid mosaic of the membrane to ensure effective passage of heme from the CWAs to the lipoprotein IsdE. It is increasingly recognized that bacterial membranes represent highly structured cellular compartments. In this regard, functional membrane microdomains (FMMs) have gained increasing attention in the recent years (**Bach and Bramkamp, 2013**; **Bramkamp and Lopez, 2015**; **Farnoud et al., 2015**; **López and Kolter, 2010**; **Matsumoto et al., 2006**; **Yokoyama and Matsui, 2020**). FMMs are specific domains in the bacterial membrane that, in the case of *S. aureus*, consist of the polyisoprenoid staphyloxanthin and its derivative lipids. An intrinsic characteristic of FMMs is the structural protein flotillin A (FloA) recruiting proteins to the FMMs and promoting their oligomerization (**Bramkamp and Lopez, 2015**; **López**

and Kolter, 2010). FMMs have been shown to be crucial to coordinate diverse cellular functions in *S. aureus*. On one hand, they control activity of cell wall biosynthetic enzymes such as PBP2a and are essential for expression of resistance to β-lactam antibiotics in methicillin-resistant *S. aureus* (MRSA) (*García-Fernández et al., 2017*). On the other hand, several membrane-associated processes such as the secretion of type VII secretion effector proteins (*Mielich-Süss et al., 2017*) or the RNase Rny depend on FloA (*Koch et al., 2017*).

In this study, we have used bacterial two-hybrid assays to show direct interaction between the iron-responsive ATPase FhuC and the heme permease protein IsdF. Additionally, we have shown that Hb-dependent growth requires FhuC activity, suggesting that FhuC energizes heme transport in *S. aureus*. Moreover, the heme permease IsdF was shown to be associated with FMMs, to interact directly with FloA and to co-localize with the latter in the bacterial envelope. Accordingly, Hb-dependent proliferation was reliant on the correct formation of FMMs. Finally, we demonstrated that appropriate FMM formation is also required for Isd-dependent proliferation of *S. lugdunensis*, suggesting that FMM-dependent structuring of the membrane is crucial for the functionality of Isd systems in staphylococci.

Results

FhuC is crucial for heme-dependent proliferation of *S. aureus*

The Isd system facilitates the acquisition of heme from Hb. Heme membrane transport involves an ABC transporter consisting of the heme-specific lipoprotein (IsdE) and the transmembrane protein

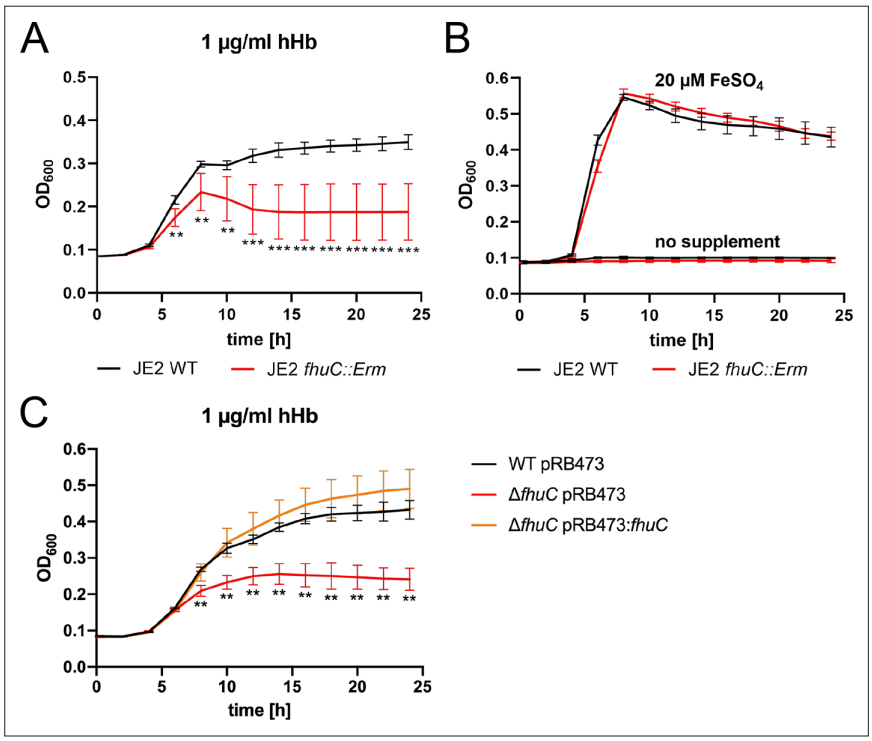

Figure 1. FhuC is needed for hemoglobin (Hb)-dependent proliferation of *S. aureus*. One-hundred µl (**A, B**) or 500 µl (**C**) of bacterial cultures were grown with human Hb or $FeSO_4$ as the sole source of iron in 96-well (**A, B**) or 48-well (**C**) format and OD_{600} was monitored over time. For reasons of clarity, values taken every 2 hr are displayed. (**A, B**) *S. aureus* USA300 JE2 wild type (WT) and USA300 JE2 *fhuC::Erm*. Means and SD of six experiments are shown. (**C**) *S. aureus* Newman Δ*fhuC* was complemented using a plasmid expressing FhuC from the native promotor (pRB473:*fhuC*). Newman WT pRB473, Δ*fhuC* pRB473, and Δ*fhuC* pRB473:*fhuC*. Means and SD of three experiments are shown. (**A, C**) Statistical analysis comparing the WT strains and the *fhuC* mutants was performed using GraphPad Prism 9 Student's unpaired t-test. **p<0.01, ***p<0.001.

The online version of this article includes the following source data for figure 1:

Source data 1. FhuC is needed for hemoglobin (Hb)-dependent proliferation of *S. aureus*.

IsdF (***Grigg et al., 2007***; ***Mazmanian et al., 2003***). Interestingly, an ATPase to energize membrane transport is not encoded within the *S. aureus isd* operon. Similarly, the operons encoding the SA and SB membrane transport systems (HtsABC and SirABC) lack intrinsic ATPases and both systems were previously shown to be energized by FhuC (***Beasley et al., 2009***; ***Speziali et al., 2006***). This ATPase is encoded within the *fhuCBG* operon allowing hydroxamate siderophore transport. Thus, FhuC appears to act as a housekeeping ATPase for iron acquisition in *S. aureus*. In order to determine if FhuC is required for heme acquisition by Isd, we studied growth of *fhuC* mutants in iron-limited medium.

We found that a *S. aureus* USA300 JE2 *fhuC::Erm* mutant, obtained from the Nebraska transposon mutant library (***Fey et al., 2013***), showed significantly reduced growth when human Hb (hHb) was supplied as a sole source of nutrient iron (***Figure 1A***). This deficit was rescued by addition of iron(II) sulfate (***Figure 1B***), suggesting that FhuC energizes heme transport across the membrane. To investigate this further, we created an isogenic deletion mutant of *fhuC* (Δ*fhuC*) in *S. aureus* strain Newman. Again, the *fhuC*-deficient strain showed a pronounced growth deficit in the presence of Hb. Importantly, plasmid-based expression of FhuC restored Hb-dependent growth (***Figure 1C***). This supports the idea that FhuC is needed for Isd-dependent heme acquisition.

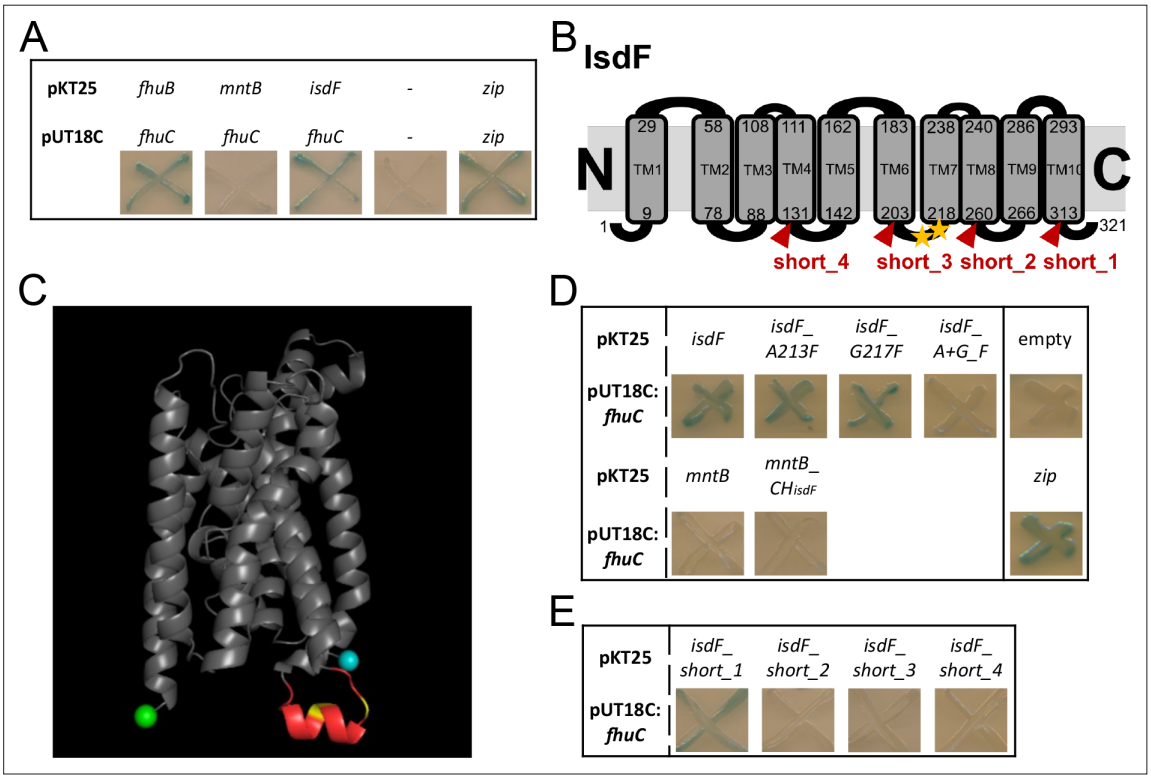

Figure 2. FhuC interacts directly with IsdF. (**A, D, E**) *Escherichia coli* BTH101 was co-transformed with pUT18C:*fhuC* and pKT25 vectors expressing permeases of interest. Where protein-protein interactions occur, the T25 and T18 catalytic domains of adenylate cyclase dimerize forming an active enzyme which produces cAMP. This activates LacZ expression leading to X-Gal degradation and blue signals on indicator plates. (**A**) Positive control, leucine zippers (zip). Negative control, empty vectors (pKT25+pUT18C) (-). (**B**) Schematic representation of the IsdF topology prediction using TOPCONS. The amino acids marking the transmembrane domains (TM) are shown with the conserved A213 and G217 indicated by yellow asterisks. Truncations are indicated in red. (**C**) IsdF structure prediction using Alphafold with visualization using PyMOL. The coupling helix is shown in red with the conserved A231 and G217 in yellow. The N-terminus is in cyan and the C-terminus in green. (**D**) Bacterial adenylate cyclase two-hybrid (BACTH) analysis of FhuC and IsdF with single and double amino acid substitutions as well as with the MntB_CH_{isdF} fusion protein (coupling helix IsdF). (**E**) BACTH analysis of FhuC and truncated IsdF derivatives.

The online version of this article includes the following source data and figure supplement(s) for figure 2:

Source data 1. FhuC interacts directly with IsdF.

Figure supplement 1. FhuC interaction with iron permeases and topology predictions.

Figure supplement 1—source data 1. FhuC interaction with iron permeases and topology predictions.

Conserved amino acids in the coupling helix of IsdF promote the interaction with FhuC

We used the bacterial adenylate cyclase two-hybrid system (BACTH) to determine whether FhuC physically interacts with the Isd permease IsdF. In BACTH, putatively interacting proteins are fused to domains of an adenylate cyclase. Interaction of the two proteins reconstitutes adenylate cyclase which allows expression of β-galactosidase (LacZ). Co-expression of FhuC with its native permease FhuB as well as with IsdF generated distinct positive signals (***Figure 2A***). In contrast, co-expression of FhuC with the iron-independent permease MntB (manganese uptake) did not result in detectable LacZ activity (***Figure 2A***). Quantification of LacZ activity confirmed the plate-based screening (***Figure 2—figure supplement 1A***). This suggests that FhuC energizes the heme transport system IsdEF and structural characteristics within the permease must allow discrimination of FhuC targets and non-targets.

ATPases and their respective permeases display Q-loops and coupling helixes, respectively, to mediate their interaction (***Hollenstein et al., 2007***; ***Wen and Tajkhorshid, 2011***). We speculated that conserved motifs within the coupling helixes of iron compound permeases might promote their energization by FhuC. To investigate this, we modeled the topology of the permease IsdF using TOPCONS (***Tsirigos et al., 2015***) and Alphafold (***Jumper et al., 2021***; ***Varadi et al., 2022***). This resulted in prediction of 10 transmembrane helices. Both the N- and C-termini of the protein as well as four loops were proposed to be located in the cytoplasm (***Figure 2B***, ***Figure 2—figure supplement 1B***). The third cytoplasmic loop (aa 204–217) contained the cytosolic coupling helix (***Figure 2B+C***). To identify motifs that might determine energization by FhuC, we aligned the sequences of the coupling helixes of all putative FhuC interaction partners (IsdF, FhuB, FhuG, SirB, SirC, HtsB, HtsC), as well as of MntB, using Clustal Omega (***Madeira et al., 2022***). This analysis showed that within all putative coupling helixes only a single glycine residue (G217 in IsdF) is conserved. Additionally, a single alanine residue (A213 in IsdF) was conserved in all iron compound permeases but not in MntB (***Figure 2B+C***, ***Figure 2—figure supplement 1C***). Many coupling helices contain an EAAxxxGxxxxxxxxxIxLP (EAA) motif (***ter Beek et al., 2014***). We speculated that the AxxxG motif identified in the iron permeases might be important to mediate interaction with FhuC. Exchange of the alanine 213 to the bulky amino acid phenylalanine (A213F) did not prevent interaction with FhuC. The same was true when glycine 217 was exchanged for phenylalanine (G217F). However, combination of both substitutions abrogated the interaction (***Figure 2D***). These results show the importance of A213 and G217 for the recognition of FhuC, but they do not explain how MntB and IsdF are discriminated. To examine this, we inserted the full-length coupling helix of IsdF at the appropriate position within MntB. Interestingly, the resulting fusion protein remained negative in BACTH analysis with FhuC (***Figure 2D***), suggesting that the sequence and structure of the coupling helix alone is not sufficient to allow FhuC to discriminate between IsdF and MntB. To further investigate this, we created a series of C-terminal truncations of IsdF (***Figure 2B+E***). Deletion of the C-terminal cytoplasmic domain (short_1) did not affect the interaction with FhuC. However, truncation at the fourth cytosolic loop (short_2) abrogated the interaction and the same was true for additional truncations lacking more extended C-terminal fragments (short_3/short_4) (***Figure 2E***). These data indicate that besides the coupling helix, the C-terminal part of IsdF is crucial for appropriate formation of the IsdF-FhuC complex.

IsdF is located within FMMs and interacts with FloA

FMMs and the associated structuring protein FloA promote the correct structure of membrane-associated proteins and protein complexes in *S. aureus* (***Bramkamp and Lopez, 2015***). Proteomic profiles of FMM-membrane fractions have been recorded previously and FMM-associated proteins were identified (***García-Fernández et al., 2017***). Revisiting these datasets showed that a high number of iron uptake-associated proteins are enriched in the FMM-containing membrane fraction including the heme transport system IsdEF and the siderophore transporters Fhu, Hts, and Sir.

To investigate further the subcellular localization of IsdF, we generated a *S. aureus* Newman strain that constitutively expresses IsdF with a triple FLAG tag. The cell membrane was isolated and non-ionic detergents were used to collect FMMs, which accumulate in the detergent-resistant membrane (DRM) fraction compared to the detergent-sensitive membrane (DSM) fraction (***Bramkamp and Lopez, 2015***; ***Brown, 2002***; ***Shah and Sehgal, 2007***). The abundance of proteins in general appeared to be slightly increased in the DSM fraction (***Figure 3A***). In contrast, quantitative western blotting showed

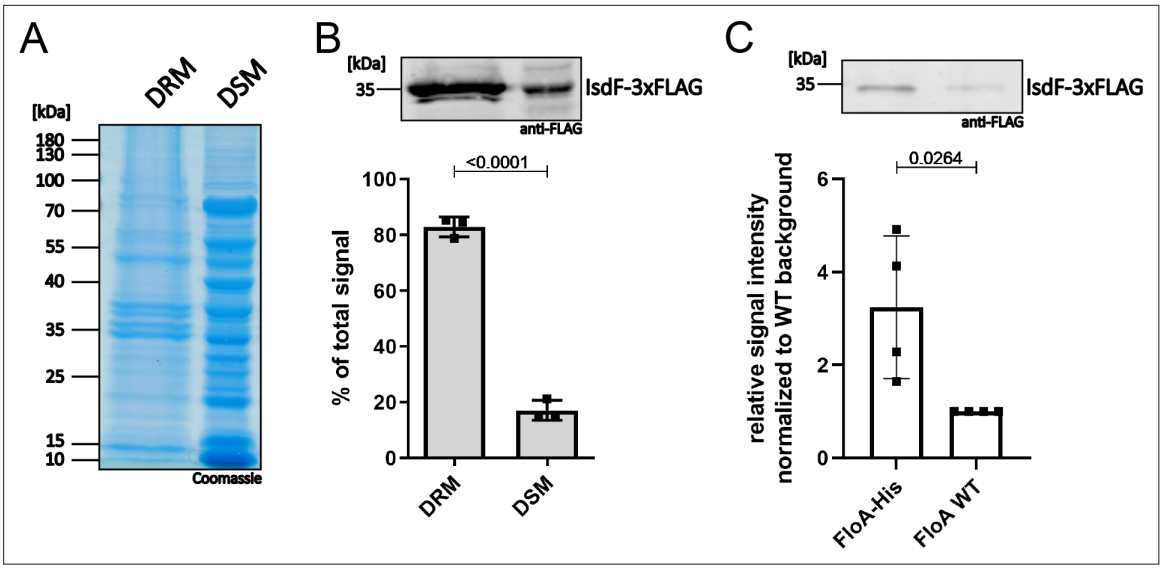

Figure 3. IsdF localizes within functional membrane microdomains (FMMs) and interacts directly with flotillin A (FloA). *S. aureus* Newman FloA-His pRB474:*isdF-3xFLAG* membranes were isolated and (**A, B**) separated into detergent-resistant membrane (DRM) and detergent-sensitive membrane (DSM) fractions or (**C**) solubilized with 1% *n*-dodecyl-β-D-maltopyranosid (DDM) overnight and co-precipitated using Ni-NTA affinity chromatography. (**A**) Coomassie blue-stained gel of DRM and DSM fractions (equal amounts loaded). (**B**) Immunoblot analysis and quantification of IsdF in DRM and DSM fractions using anti-FLAG antibody and LI-COR infrared technology. An example of the IsdF-3xFLAG bands in the DRM and DSM fractions is shown. Quantification of signals were calculated as a percentage of the total signal (DRM+DSM). Means and SD of three independent experiments are shown. (**C**) Co-precipitation analysis using anti-FLAG antibody for detection of IsdF-3xFLAG (pRB474:*isdF-3xFLAG*) that co-eluted with FloA-His or FloA WT. An example of the IsdF-3xFLAG bands that co-eluted with FloA-His and FloA WT are shown. Quantification of FloA-His IsdF-3xFLAG signals in immunoblots was normalized to FloA WT strain signals (set to 1). Means and SD of four independent experiments are shown. Statistical analysis (Student's unpaired t-test) was performed using GraphPad Prism 8.

The online version of this article includes the following source data and figure supplement(s) for figure 3:

Source data 1. IsdF localizes within functional membrane microdomains (FMMs) and interacts directly with flotillin A (FloA).

Figure supplement 1. Input control for co-immunoprecipitation of flotillin A (FloA) and IsdF.

Figure supplement 1—source data 1. Input control fro co-immunoprecipitation of flotillin A (FloA) and IsdF.

that 80% of the IsdF signal was detected in the DRM fraction (***Figure 3B***). This confirms that IsdF is predominantly associated with the DRM fraction and suggests that IsdF is localized within FMMs.

It was previously postulated that the structuring protein FloA recruits target proteins to FMMs (***Bramkamp and Lopez, 2015***; ***Lopez and Koch, 2017***). Therefore, we investigated if this is also true for IsdF. We co-expressed IsdF-triple FLAG with the FloA WT protein or with FloA tagged with hexa-histidine in *S. aureus* Newman and performed Ni-NTA affinity chromatography. Prior to Ni-NTA chromatography, IsdF was equally abundant in both strains showing equal expression (***Figure 3—figure supplement 1***). However, IsdF was three times more abundant in the Ni-NTA eluate of the FloA-His expressing strain (***Figure 3C***). This strongly suggests that IsdF interacts with FloA which allows co-purification. Low levels of IsdF-triple FLAG were detected within the eluate of the FloA WT expressing strain, suggesting minor non-specific interaction of either IsdF or FloA with the Ni-NTA column.

FloA and IsdF are spatially coordinated in intact cells

We used fluorescent microscopy to investigate the localization of FloA and IsdF in intact cells of *S. aureus* Newman. The IsdF protein was tagged by mNeongreen while FloA was coupled to SNAP. The latter was visualized by addition of TMR. As described previously, FloA signals formed distinct foci at the bacterial surface most likely representing FMMs (***Figure 4A***). Interestingly, IsdF also accumulated in patches (***Figure 4A***). However, visual inspection indicated that the IsdF and FloA signals did not necessarily overlap perfectly but rather seemed to be in close proximity. We assessed this observation systematically by measuring the distance between proximal fluorescent maxima of IsdF and FloA in hundreds of individual cells (***Figure 4B***). This showed a perfect overlap in 7.5% of measurements while maxima were separated by a single pixel (0.0645 µM) or by two pixels (0.129 µM) in 29.5% and 26.7%

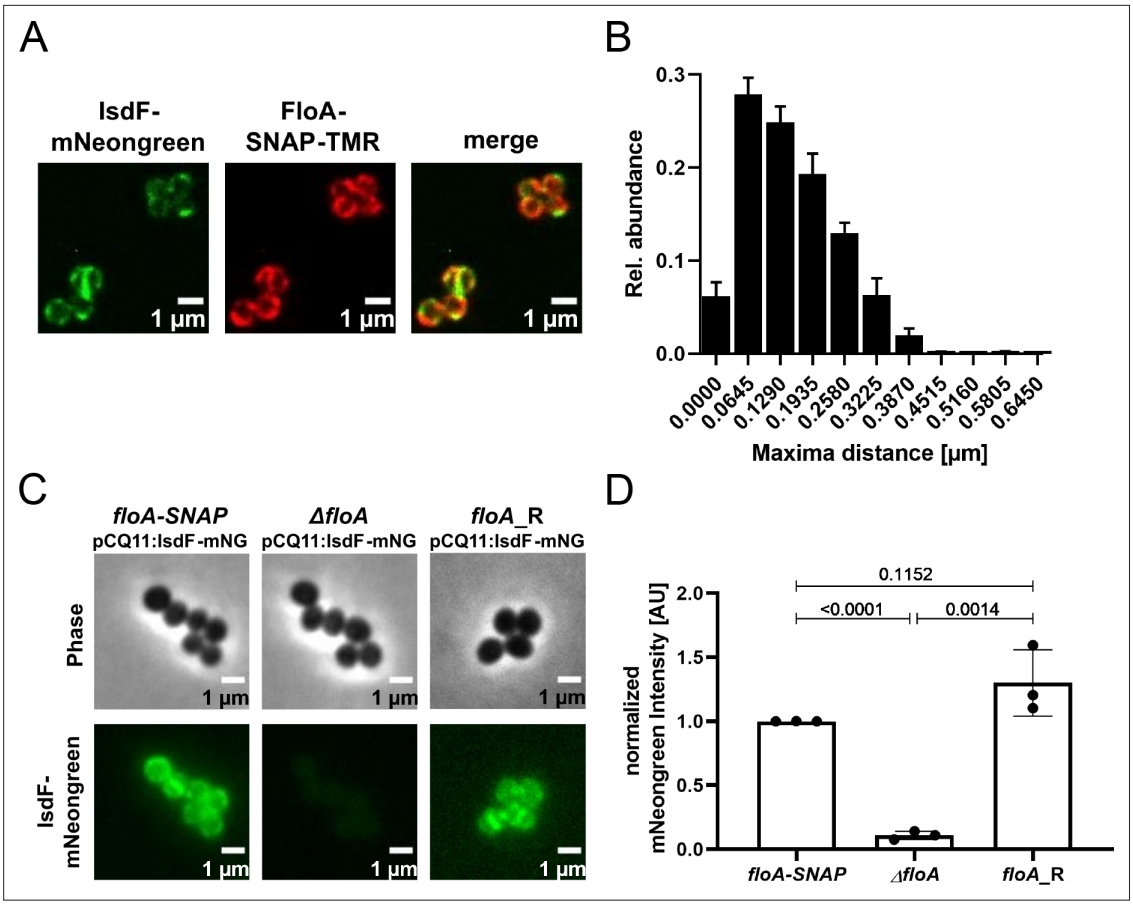

Figure 4. Flotillin A (FloA) is crucial for spatial organization of IsdF in the membrane of *S. aureus*. (**A**) Examples of a fluorescence micrograph of *S. aureus* Newman *floA-SNAP* pCQ11:*isdF-mNeongreen*. Green: IsdF-mNeongreen. Red: FloA-SNAP-TMR. Scale bars, 1 µm. (**B**) Quantification of the proximity of IsdF-mNeongreen fluorescence maxima and FloA-SNAP-TMR fluorescence maxima. The distance of each FloA-SNAP-TMR maximum to the nearest IsdF-mNeongreen maximum was measured with pixel (px) accuracy (1 px=0.0645 µm). The histogram shows the relative distribution of determined distances. Bars show means and SD of three independent biological replicates. Total number of maxima measured was n≥876 per replicate for each labeled protein. n≥293 cells per replicate. (**C**) An example of a fluorescence micrograph of *S. aureus* Newman *floA-SNAP* pCQ11:*isdF-mNeongreen*, *ΔfloA* pCQ11:*isdF-mNeongreen*, and *floA*_R pCQ11:*isdF-mNeongreen*. Scale bars, 1 µm. (**D**) Quantification of IsdF-Neongreen fluorescence intensity of individual cells. The bar shows the means and SD of three independent biological experiments. n≥241 cells analyzed per strain. Data was normalized to the respective FloA-SNAP replicate mean. Statistical significance was determined using unpaired two-tailed Student's t-test with 95% confidence interval.

The online version of this article includes the following source data for figure 4:

Source data 1. Flotillin A (FloA) is crucial for spatial organization of IsdF in the membrane of *S. aureus*.

of cases, respectively. The number of maxima within a certain distance group declined with increasing distance. Maxima that were further apart than 0.3225 µM were rarely detected. Furthermore, we found that fluorescent signals derived from plasmid pCQ11:*isdF-mNeongreen* were strong in a FloA expressing strain but almost undetectable in a *floA*-deficient mutant (***Figure 4C+D***). Replacement of the mutant allele with the functional WT allele (Newman *floA*_R) by allelic exchange restored IsdF signals to WT level (***Figure 4C+D***). These data suggest that FloA is crucial for the appropriate incorporation and spatial distribution of IsdF within the membrane of *S. aureus*.

FloA and appropriately formed FMMs are needed for bacterial growth using Hb as the sole iron source

The full functionality of membrane-associated protein complexes in *S. aureus* requires both FMMs and FloA (***García-Fernández et al., 2017***; ***Koch et al., 2017***; ***Mielich-Süss et al., 2017***). Due to the location of IsdF within FMMs, we hypothesized that appropriately formed FMMs would be relevant

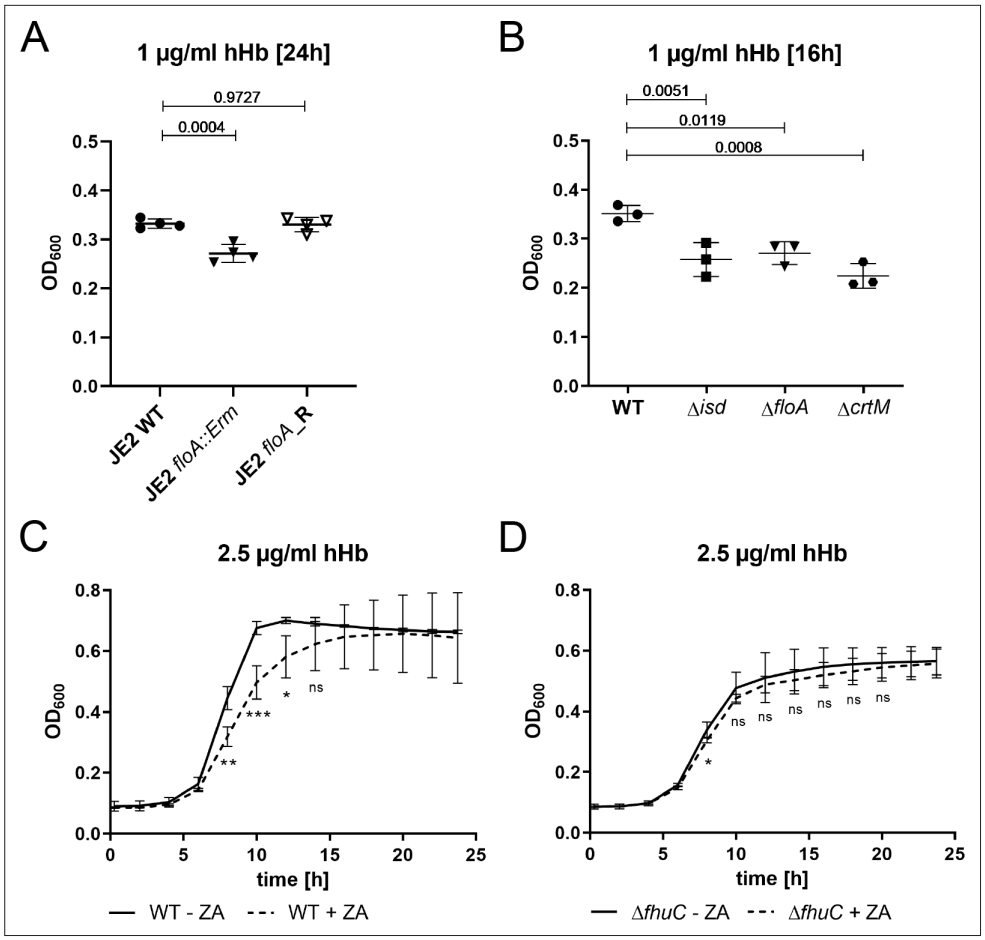

Figure 5. Flotillin A (FloA) and functional membrane microdomains (FMMs) are needed for proliferation with hemoglobin. (**A–D**) Strains were grown in iron-limited medium (A: 100 µl in 96-well plates; B–D: 500 µl in 48-well plates). (**A**) Growth of *S. aureus* USA300 JE2 WT, Δ*floA::Erm* and *floA*_Revertant (*floA_R*) in the presence of 1 µg/ml human hemoglobin (hHb). For reasons of clarity, values after 24 hr are displayed. Means and SD of four experiments are shown. (**B**) Growth of *S. aureus* Newman WT, Δ*isd*, Δ*floA,* and Δ*crtM* mutants. Strains were grown in the presence of 1 µg/ml hHb. Values after 16 hr are displayed. Means and SD of three experiments are shown. (**C,D**) Newman WT (**C**) and Δ*fhuC* (**D**) were grown in the presence of 10 µM zaragozic acid (ZA) and 2.5 µg/ml hHb. Values taken every 2 hr are displayed. Means and SD of four experiments are shown. (**A,B**) Statistical analysis: Student's one-way ANOVA followed by Dunett's test for multiple comparisons was performed using GraphPad Prism 9. (**C,D**) Statistical analysis: Student's unpaired t-test was performed using GraphPad Prism 8. *p<0.05, **p<0.01, ***p<0.001.

The online version of this article includes the following source data and figure supplement(s) for figure 5:

Source data 1. Flotillin A (FloA) and functional membrane microdomains (FMMs) are needed for proliferation with hemoglobin.

Figure supplement 1. $FeSO_4$ growth controls of *floA* and functional membrane microdomain (FMM)-deficient mutants.

Figure supplement 1—source data 1. $FeSO_4$ growth controls of *floA* and functional membrane microdomain (FMM)-deficient mutants.

for staphylococcal iron acquisition. First, we tested this using a USA300 JE2 *floA:Erm* mutant derived from the Nebraska transposon mutant library. Growth in the presence of $FeSO_4$ was not impacted by this mutation (***Figure 5—figure supplement 1A***), but a significant growth reduction was observed when Hb was supplied as the sole source of nutrient iron. Replacement of the mutant allele with the functional WT allele (JE2 *floA*_R) by allelic exchange restored full growth (***Figure 5A***). These data support the idea that FloA-dependent incorporation of IsdF is needed for heme acquisition.

Next, we validated the importance of FMMs for heme acquisition also for *S. aureus* Newman. We created three mutant strains lacking (i) the entire Isd system (Δ*isd*), (ii) FloA (Δ*floA*), and (iii) squalene synthase CrtM (Δ*crtM*) which results in FMM deficiency due to the inability to synthesize polyisoprenoid lipids (***Liu et al., 2012***; ***López and Kolter, 2010***). All mutants showed WT levels of growth in the presence of $FeSO_4$ (***Figure 5—figure supplement 1B***) but had a comparable growth deficit in the presence of Hb (***Figure 5B***). Additionally, blockage of FMM biosynthesis by zaragozic acid (ZA) (***López and Kolter, 2010***) reduced Hb-dependent growth (***Figure 5C***). Importantly, the reduced growth of the *fhuC* mutant was not further decreased by the addition of ZA (***Figure 5D***), suggesting that impaired iron acquisition and not any toxic effects of ZA were responsible for the growth defects in the WT strain. In addition, ZA did not affect growth in the presence of $FeSO_4$ (***Figure 5—figure supplement 1C+D***). All these experiments suggest that functional FMMs are crucial for Hb usage by *S. aureus*.

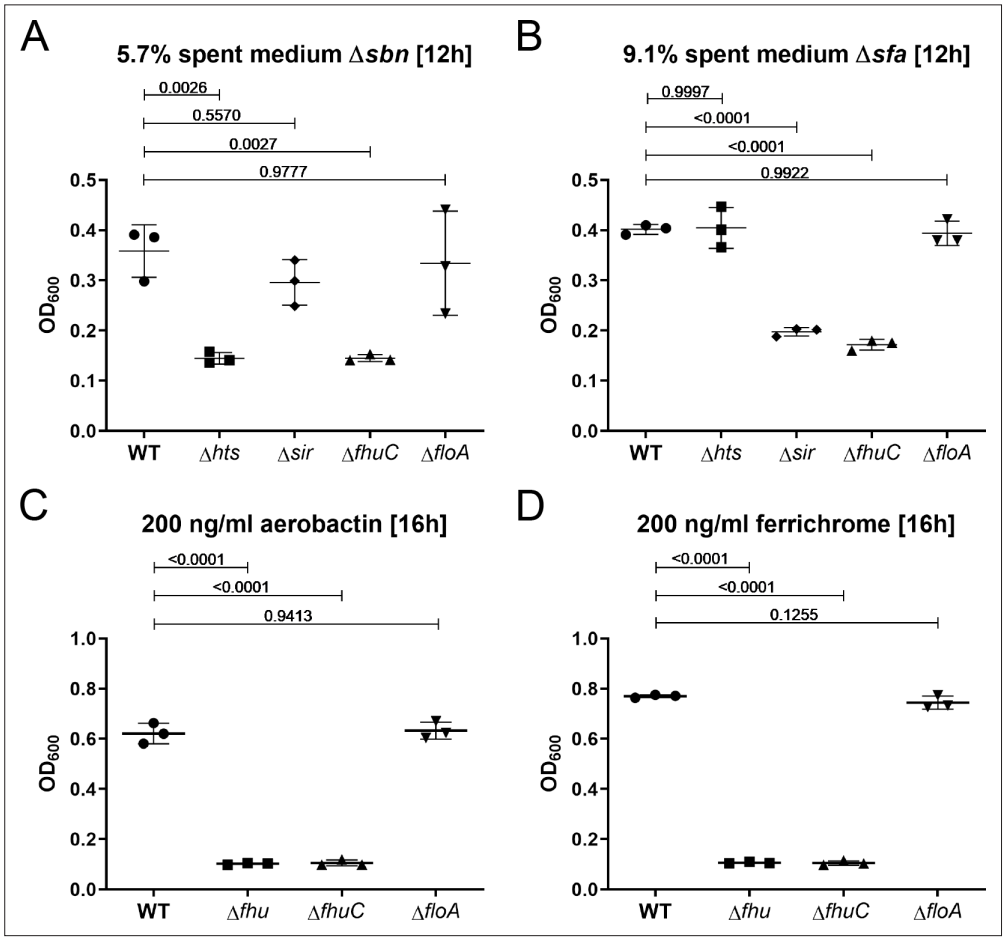

Figure 6. Growth using siderophores is independent of functional membrane microdomains (FMMs). Newman WT, Δ*htsABC*, Δ*sirABC*, Δ*fhuCBG*, Δ*fhuC*, and Δ*floA* were grown in the presence of 5.7% spent medium of *S. aureus* USA300 JE2Δ*sbn* (containing staphyloferrin A) (**A**), 9.1% spent medium of USA300 JE2 Δ*sfa* (containing staphyloferrin B) (**B**), 200 ng/ml aerobactin (**C**) or 200 ng/ml ferrichrome (**D**). Strains were grown in 500 µl of iron-limited medium in 48-well plates. For reasons of clarity, values after 12 hr (**A, B**) or 16 hr (**C, D**) are displayed. Means and SD of three experiments are shown. Statistical analysis: Student's one-way ANOVA followed by Dunett's test for multiple comparisons was performed using GraphPad Prism 9.

The online version of this article includes the following source data and figure supplement(s) for figure 6:

Source data 1. Growth using siderophores is independent of functional membrane microdomains (FMMs).

Figure supplement 1. $FeSO_4$ growth controls of iron transporter and *floA* mutants.

Figure supplement 1—source data 1. $FeSO_4$ growth controls of iron transporter and *floA* mutants.

We also found proteins of the siderophore acquisition systems Hts, Sir, and Fhu, to be enriched in the proteomic profile of FMM-membrane fractions (***García-Fernández et al., 2017***). Therefore, we investigated if FloA is also relevant for siderophore acquisition. We created individual mutants of all three systems in *S. aureus* Newman and compared growth of the mutants to that of the *floA* mutant in the presence of SA, SB, or the hydroxamate siderophores aerobactin and ferrichrome. As a source of SA and SB, dilute culture supernatant of *S. aureus* USA300 JE2 Δ*sbn* (secreting only SA) and *S. aureus* USA300 JE2 Δ*sfa* (secreting only SB) was used, respectively. All mutants showed WT levels in the presence of $FeSO_4$ (***Figure 6—figure supplement 1A+B***). The Δ*htsABC* and Δ*sirABC* mutants showed growth deficiency in the presence of SA and SB (***Figure 6A+B***), respectively, and Δ*fhuCBG* failed to grow in the presence of aerobactin and ferrichrome (***Figure 6C+D***). The *fhuC* mutant showed growth deficiency with all siderophores tested (***Figure 6A–D***). These data are in agreement with previous datasets (***Beasley et al., 2009***; ***Cheung et al., 2009***; ***Sebulsky et al., 2000***; ***Speziali et al., 2006***). However, the Δ*floA* mutant did not show any growth deficits compared to the WT strain under the tested conditions (***Figure 6A–D***). This data suggests that in contrast to acquisition of Hb-derived heme, acquisition of siderophores is not dependent on membrane structuring by FMMs.

Sortase function does not depend on FloA and FMMs

A major difference between the heme membrane transporter IsdEF and all siderophore transport systems is that IsdEF relies on CWAs (IsdA, IsdB, IsdH, IsdC) to extract heme from Hb and to funnel it over the cell wall to the membrane transporter (***Mazmanian et al., 2003***). In contrast, siderophores diffuse freely to the cell membrane. CWAs are anchored to the cell wall by the action of sortases (***Marraffini et al., 2006***). Intriguingly, when we reanalyzed the FMM proteomic datasets of García-Fernández and colleagues, we found both sortases of *S. aureus* (sortase A [SrtA] and sortase B [SrtB]) to be enriched within the FMM fraction (***García-Fernández et al., 2017***). Accordingly, it seemed possible that the Hb-dependent growth defects of FMM and *floA* mutants might in part result from impaired sorting of CWA Isd proteins which could hinder heme extraction and funneling. To investigate this, we assessed the functionality of the housekeeping SrtA by studying the cellular localization of its substrate IsdA. We separated cell wall and membrane fractions of various strains and detected IsdA by western blotting. As reported earlier (***Mazmanian et al., 2003***), IsdA was localized in the cell wall fraction of *S. aureus* WT. In the *srtA* mutant, the protein was exclusively detected in the membrane fraction (***Figure 7***). Interestingly, neither inactivation of FloA nor of CrtM resulted in mislocalization of IsdA (***Figure 7***). These data show that sorting of IsdA is independent of FMMs, suggesting general functionality of the sortases.

FloA is needed for Isd-dependent Hb usage in *S. lugdunensis*

As Isd systems are found in several staphylococcal species (***Heilbronner et al., 2016***; ***Mazmanian et al., 2003***; ***Sun et al., 2020***), we investigated if the involvement of FMMs and flotillins in heme uptake via the Isd system is a general concept. *S. lugdunensis* encodes for an Isd system similar to that of *S. aureus* (***Heilbronner et al., 2011***; ***Heilbronner et al., 2016***). However, in addition to the Isd system, *S. lugdunensis* encodes the energy coupling factor-type heme transporter LhaSTA

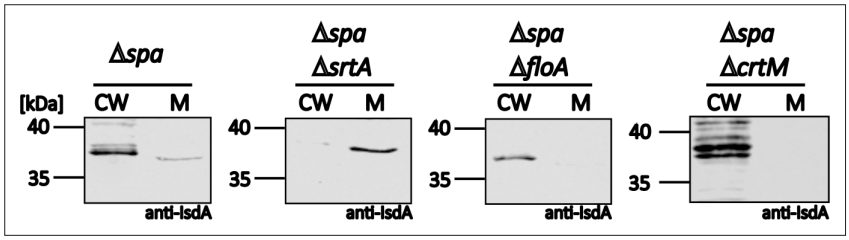

Figure 7. Sortase function does not depend on functional membrane microdomains (FMMs). *S. aureus* Newman Δ*spa*, Δ*spa*Δ*srtA::Erm*, Δ*spa*Δ*floA::Erm*, and Δ*spa*Δ*crtM::Erm* cells were grown in iron-limited medium and treated with lysostaphin to gain cell wall (CW) and membrane (**M**) fractions. Fractions were analyzed by SDS-PAGE and western blotting. IsdA was detected using polyclonal anti-IsdA antibodies.

The online version of this article includes the following source data for figure 7:

Source data 1. Sortase function does not depend on functional membrane microdomains (FMMs).

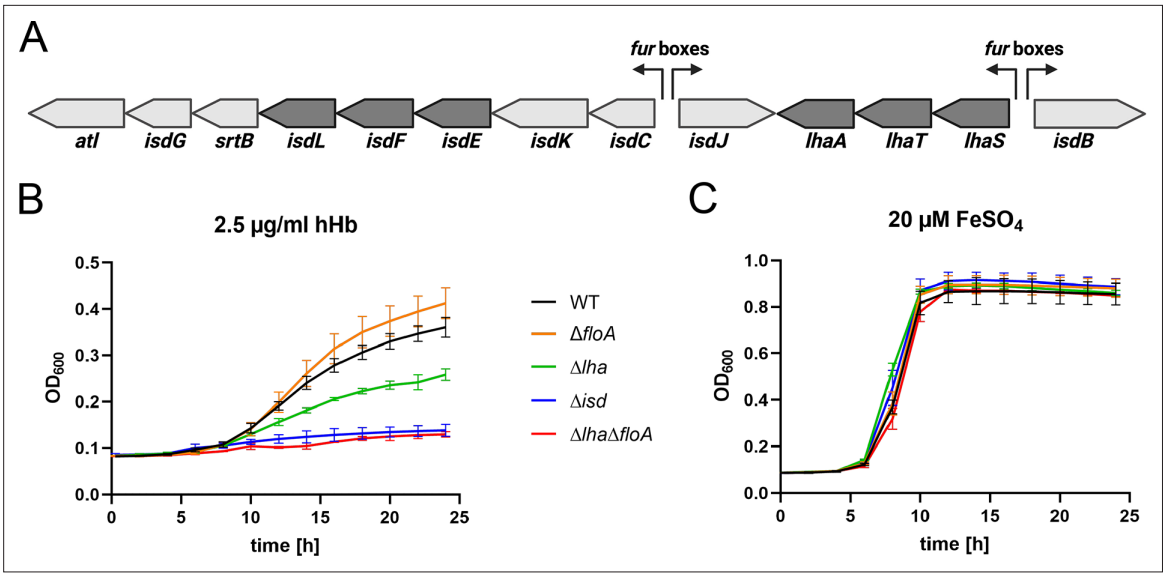

Figure 8. Flotillin A (FloA) is needed for iron-regulated surface determinant (Isd)-dependent proliferation in *S. lugdunensis*. (**A**) Schematic representation of the *isd* locus in *S. lugdunensis* N920143. Membrane transporters IsdEFL and LhaSTA in dark gray. Fur boxes are indicated. This figure was created with https://www.biorender.com/. (**B, C**) *S. lugdunensis* N920143 WT, Δ*floA*, Δ*lha*, Δ*isd*, and Δ*lha*Δ*floA* were grown in 500 µl of iron-limited medium in the presence of 2.5 µg/ml human hemoglobin (hHb) (**B**) or 20 µM $FeSO_4$ (**C**) as the sole source of iron in 48-well plates. Values taken every 2 hr are displayed. Means and SD of three experiments are shown.

The online version of this article includes the following source data for figure 8:

Source data 1. Flotillin A (FloA) is needed for iron-regulated surface determinant (Isd)-dependent proliferation in *S. lugdunensis*.

(***Jochim et al., 2020***; ***Figure 8A***). Inactivation of *lhaSTA* in *S. lugduneneis* N920143 resulted in a significant reduction of Hb-dependent growth but only deletion of the entire *isd* locus (*atl* to *isdB* including *lhaSTA*) abrogated growth completely (***Figure 8B***). Accordingly, growth of the Δ*lhaSTA* mutant reflects Isd-dependent proliferation in *S. lugdunensis*. We identified a single FloA homologue (SLUG_13380) in *S. lugdunensis*. Inactivation of *floA* in the Δ*lhaSTA* background resulted in complete abrogation of Hb-dependent growth (***Figure 8B***), showing the importance of functional FMMs for Isd-dependent heme in this species, too. Interestingly, inactivation of *floA* in *S. lugdunensis* WT did not influence Hb-dependent growth, suggesting that activity of LhaSTA does not depend on FMMs and allows inhibition of the Isd system to be by-passed. All mutants showed WT levels of growth in presence of $FeSO_4$ (***Figure 8C***).

Discussion

ABC transporters are classical molecular machines that transport nutrients across biological membranes and allow their accumulation against concentration gradients at the cost of ATP (***Rees et al., 2009***). Prokaryotic ABC-type importers consist of three functionally distinct subunits, an extracellular substrate-binding protein (SBP), a membrane-located permease and a cytosolic ATPase. In Gram-negative bacteria, SBPs are located in the periplasmic space while the SBPs of Gram-positive bacteria are lipoproteins that are coupled to the extracellular leaflet of the membrane. SBPs bind the target substrate and deliver it to the membrane. The membrane permeases consist of two subunits (homo- or heterodimers) and promote translocation of the substrate. The ATP-binding protein binds to the permease and energizes transport of the substrate by hydrolysis of ATP (***Dassa and Bouige, 2001***; ***Locher, 2009***; ***Zolnerciks et al., 2011***). It is known that a single ATPase can energize several permeases with different substrates (***Quentin et al., 1999***) including the iron compound permeases of *S. aureus*. *S. aureus* possesses genes for biosynthesis of the siderophores SA and SB (***Beasley et al., 2009***; ***Cheung et al., 2009***; ***Cotton et al., 2009***). However, the loci encoding their respective importers do not express an ATPase. It has been shown that FhuC, the ATPase encoded within the hydroxamate siderophore transport system *fhuCBG*, is needed for staphyloferrin-dependent proliferation (***Beasley et al., 2009***; ***Sebulsky et al., 2000***; ***Speziali et al., 2006***). The *isd* operon of *S. aureus* also lacks a

gene encoding an ATPase. Here, we show that deletion of *fhuC* has a major impact on Hb-dependent growth. This suggests that FhuC is a housekeeping ATPase that powers acquisition of different iron compounds by *S. aureus*. However, weak Hb-dependent growth was observed with the Δ*fhuC* mutant. This could indicate that an unknown ATPase partially substitutes for the function of FhuC. Such an exchangeability of ATPases was previously described (**Hekstra and Tommassen, 1993**; **Leisico et al., 2020**; **Webb et al., 2008**). Seven ABC iron compound transporters were previously identified in the genome of *S. aureus* (Sst, Fhu, Sir, Hts, Isd systems, SAUSA300_1514–1517 and SAUSA300_0598–99) with SstC and SAUSA300_1516 being ATPases besides FhuC (**Skaar et al., 2004**). It seems possible that these are able to partly substitute for FhuC. However, further experiments are needed to validate this. Alternatively, a secondary heme transporter might exist in *S. aureus*. It is worth considering that Isd-dependent heme acquisition in other pathogens appears to be energized by specialized ATPases. This has been experimentally proven for *S. lugdunensis* where the ATPase IsdL (**Heilbronner et al., 2011**) energizes heme transport by IsdEF (**Flannagan et al., 2022**). Similarly, the *isd* loci of *B. anthracis* (**Skaar et al., 2006**), *B. cereus* (**Abi-Khalil et al., 2015**), and *L. monocytogenes* (**Jin et al., 2006**; **Klebba et al., 2012**) possess genes encoding putative ATPases. However, the relevance of these ATPases for heme acquisition lacks experimental validation. Nevertheless, it seems plausible that they are required to energize heme membrane transport in these organisms.

All available knowledge indicates that FhuC functions as a housekeeping ATPase that energizes at least four different iron compound transporters ($FhuCBGD_1D_2$, SirABC, HtsABC, and IsdEF). Similar cases of ATPases energizing a variety of importers have been reported for other species such as *Streptococcus pneumoniae* (**Linke et al., 2013**; **Marion et al., 2011**), *Streptococcus suis* (**Tan et al., 2015**), *Streptomyces reticuli* (**Schlösser, 2000**), *Streptomyces lividans* (**Hurtubise et al., 1995**), and *Bacillus subtilis* (**Ferreira et al., 2017**; **Ferreira and Sá-Nogueira, 2010**; **Morabbi Heravi et al., 2019**; **Schönert et al., 2006**). All these systems are carbohydrate type I importers while those energized by FhuC are type II importers. Type I importers typically have permeases with only six transmembrane domains (TMDs) and acquire substrates like ions, amino acids, and sugars. In contrast, type II importer permeases consist of 10 TMDs and take up bigger substrates like heme or cobalamin (**Locher, 2009**). However, precise structural motifs that allow interactions between an ATPase and multiple different permeases remain widely elusive. ATPases and permeases interact using Q-loops and coupling helices, respectively (**Hollenstein et al., 2007**; **Locher, 2009**). Coupling helices often contain an EAA motif to facilitate interaction with an ATPase (**ter Beek et al., 2014**). A classical EAA motif is not apparent within the coupling helices of FhuB, FhuG, HtsB, HtsC, SirB, SirC, and IsdF. However, we identified conserved alanine and glycine residues that in combination are necessary for interaction with FhuC, which suggests that these residues are of crucial importance for targeting FhuC. Besides conserved amino acids, the secondary structures of coupling helices are important for the recruitment of ATPases (**Beis, 2015**; **Hollenstein et al., 2007**; **Locher, 2009**). However, the full-length coupling helix of IsdF, when inserted into MntB, did not allow MntB to interact with FhuC. This suggests that additional molecular signatures enable FhuC to identify appropriate interaction partners. Interestingly, deletion of the C-terminal part of IsdF including the fourth cytosolic loop prevented interaction with FhuC. It is possible that truncation of the C-terminal part of IsdF prevents appropriate folding or homodimerization, which might inhibit appropriate interaction with the ATPase. Nevertheless, it is also possible that in addition to a matching coupling helix, interaction between C-terminal residues of IsdF and FhuC is needed to stabilize binding. Further experiments to investigate the molecular structure of the protein complexes by X-ray crystallography are needed to validate this hypothesis.

Interestingly, components of all FhuC-energized transporters are associated with the DRM fraction of *S. aureus* membranes, suggesting that they are integrated in FMMs. FMMs were previously shown to be important for the oligomerization of cell wall biosynthetic enzymes like PBP2a (**García-Fernández et al., 2017**), for the function of membrane-bound protein complexes like the type VII secretion system (**Mielich-Süss et al., 2017**) and the RNase Rny, which is part of the degradosome (**Koch et al., 2017**) in *S. aureus*. A role for FMMs in nutrient acquisition has not been described previously. Many different ABC transporters are present in the proteomic profile of FMM-membrane fractions, for example components of magnesium (MgtE), manganese (MntH), molybdenum (ModA), phosphate (PitA), oligopeptide (OppB, OppC), and fructose (FruA) transporters (**García-Fernández et al., 2017**). It is unclear if this is the result of biochemical characteristics that are shared between membrane proteins or if this association is promoted by the FMM scaffolding protein FloA and is

important for import of nutrients. Here, we showed that FloA directly interacts with the permease IsdF, supporting the idea of active integration of permeases into FMMs. If this holds true for other permeases remains to be investigated. However, in the light of shared ATPases it is tempting to speculate that active integration into FMMs can create spatial proximity between permeases and improve the recruitment of energizing proteins such as FhuC to optimize functionality. It is possible that FloA facilitates oligomerization of larger complexes consisting of multiple permeases that are collectively energized. However, we found that disruption of FMMs by mutation of *floA* interfered with Isd-dependent proliferation but not siderophore-dependent growth. Similarly, we found that the function of sortase is not impaired in a *floA*-deficient mutant. This indicates that active integration into FMMs is not occurring for all proteins identified by DRM/DSM analysis in membrane extracts. But it is clearly occurring and functionally relevant for some of them.

Previously, treatment with ZA was shown to reduce *S. aureus* virulence in vitro and in vivo (***García-Fernández et al., 2017***; ***Koch et al., 2017***; ***Mielich-Süss et al., 2017***). Our data suggest that besides reducing the functionality of virulence factors, limiting the ability to overcome restriction of iron acquisition might also contribute to this phenomenon. Accordingly, statins like ZA might represent a new treatment approach to treat *S. aureus* infections by targeting diverse cellular functions simultaneously

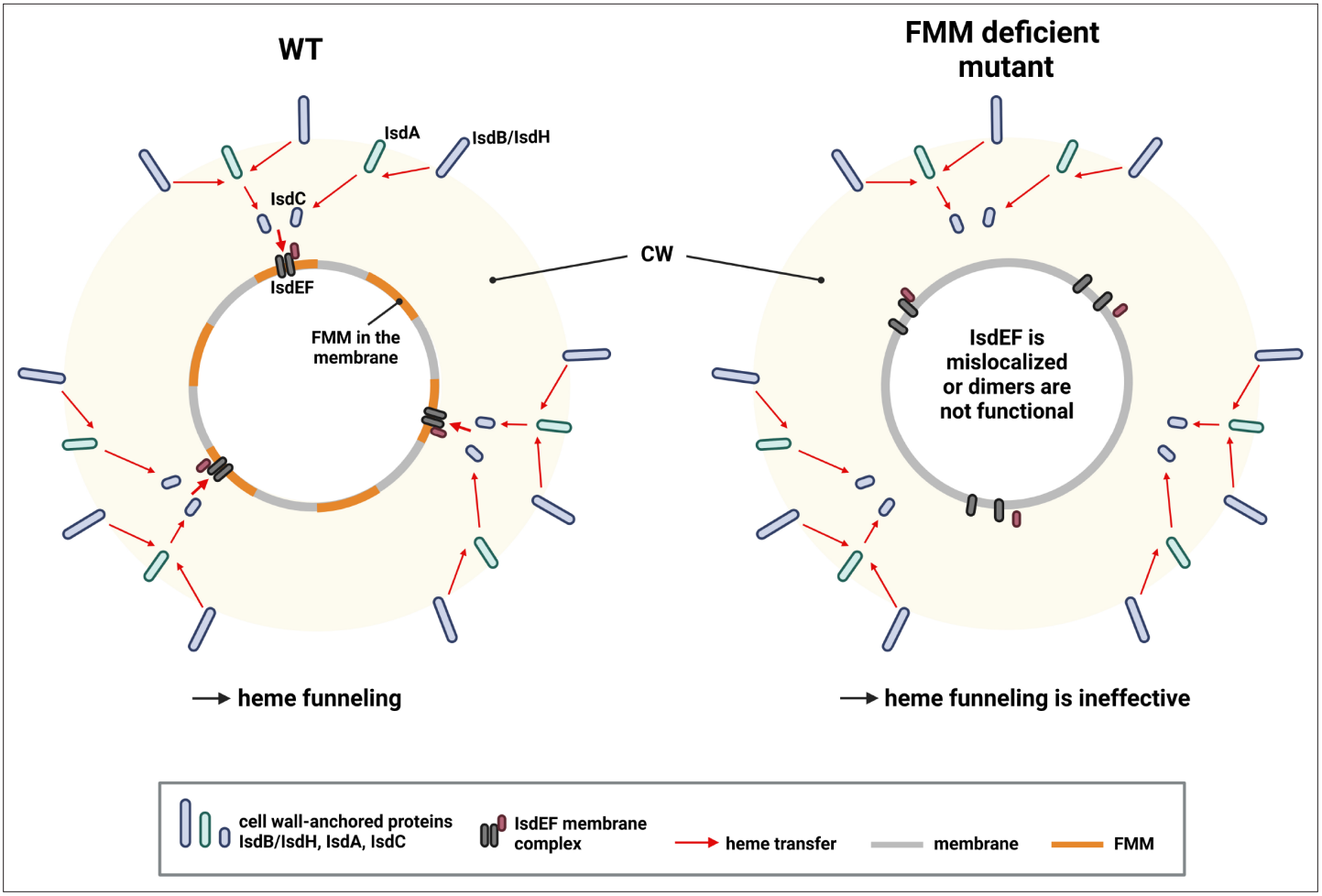

Figure 9. Proposed model of heme funneling over the *S. aureus* cell envelope. Cell wall (CW) and membrane of a *S. aureus* are shown. Heme transfer is indicated by red arrows. The surface-exposed receptors (IsdB and IsdH) extract heme from host hemoproteins and guide it to IsdA and IsdC. We propose that functional membrane microdomains (FMMs) allow structural alignment of IsdC and the membrane receptor IsdEF. Alternatively, the IsdEF complex might be unstable in an FMM or flotillin A (FloA)-deficient strain. This figure was created with https://www.biorender.com/.

The online version of this article includes the following source data for figure 9:

Source data 1. Proposed model of heme funneling over the *S. aureus* cell envelope.

and could lead to the resurrection on β-lactam antibiotics to treat MRSA infections (***Foster, 2019***; ***Somani et al., 2016***).

Speculation

It is unclear why activity of Isd depends on FMMs while siderophore transport does not. However, there must be a functional difference between the systems explaining this. Only Isd-dependent heme acquisition depends on the activity of CWAs. Interestingly, the Isd-dependent heme transport across the cell wall is structured. Hb binding and heme extraction is facilitated by the surface-exposed receptors IsdB and IsdH. Heme is then passed to IsdA and from there to IsdC. In contrast to the other cell wall-anchored molecules, IsdC is anchored by SrtB, allowing placement of the protein in the central layers of the peptidoglycan (***Mazmanian et al., 2003***; ***Mazmanian et al., 2002***). This structure is referred to as a 'heme funnel' (***Sheldon and Heinrichs, 2015***) and is thought to allow concerted passage of heme over the envelope. It seems possible that the funnel needs the heme-specific transporter IsdEF to be appropriately aligned with IsdC to allow efficient passage of heme to the membrane (***Figure 9***). Along this line, FMMs might allow alignment of IsdC and IsdEF. However, a deeper understanding of the spatial location and distribution of IsdC as well as of FMMs is needed to verify this.

Alternatively, it seems possible that FloA is crucial for formation of the IsdF homodimer within the membrane. It was previously shown that FloA deficiency reduces the formation of protein complexes in the membrane of *S. aureus* (***García-Fernández et al., 2017***; ***Koch et al., 2017***; ***Mielich-Süss et al., 2017***). Our microscopy analysis showed that IsdF-derived signals were almost indetectable within a *floA*-deficient background, which might result from an incomplete folding or homodimer formation which might entail degradation of the protein.

Materials and methods

Chemicals

If not stated otherwise, reagents were purchased from Sigma.

Bacterial strains, media, and culture conditions

The bacterial strains generated and used in this study are listed in Appendix—Key resources table. *E. coli* strains were grown in Lysogeny Broth (LB), *S. aureus* strains in TSB or RPMI+1% casamino acids (CA) (Bacto, BD Biosciences) overnight at 37°C with agitation. Antibiotics were added where appropriate: kanamycin (50 µg/ml), ampicillin (100 µg/ml), chloramphenicol (10 µg/ml), erythromycin (2.5 µg/ml).

Creation of deletion mutants, complementation, 6xHis-/3xFLAG-/SNAP-/mNeongreen-tagged strains

To create markerless deletions of *S. aureus* Newman *isd*, *fhu (fhuCBG), hts (htsABC), sir (sirABC)*, *fhuC*, *floA*, and *spa*, and of *S. aureus* USA300 JE2 Δ*sbn (sbnA-I)* and Δ*sfa (sfaA-D)*, 500 bp DNA flanking regions of the genes to be deleted were amplified from chromosomal DNA. For the genomic complementation of USA300 JE2 *floA::Erm* (*floA*_R) and Newman Δ*floA* (floA_R), 500 bp upstream with the first half of the *floA* gene and the second half of the *floA* gene and 500 bp downstream were amplified. PCR fragments were fused by overlap extension PCR and cloned into pIMAY by restriction digestion.

For the deletion of *floA* in *S. lugdunensis* N920143, we identified the *S. aureus* Newman *floA* homologue (SLUG_13380) in *S. lugdunensis* N920143 using BLAST. Five-hundred bp upstream and downstream of the gene were amplified, joint by overlap extension PCR and cloned into pIMAY.

For the creation of the C-terminally 6xHis-tagged *floA-6xHis* and SNAP-tagged *floA-SNAP* strains, the 3 500 bp of the *floA* gene as well as the 500 bp of the downstream region of *floA* stop codon were amplified by PCR. For the 6xHis-tagged strain, the primers contained a sequence overlap and in addition a linker (AGAGGATCG) and the hexa histidine encoding sequence (CATCACCATCACCATCAC) to integrate the tag before the stop codon of the *floA* gene; for the SNAP-tagged strain, the primers contained a sequence overlap for the SNAP sequence, which was amplified from pCQ11:*snap*, to integrate the tag before the stop codon of *floA*. Fragments were joint by overlap extension PCR and cloned into pIMAY using restriction digestion.

Allelic replacement was used to create staphylococcal mutants as described elsewhere (**Monk et al., 2012**).

For the complementation of Newman Δ*fhuC*, the gene including its fur box was amplified and cloned into pRB473 using restriction digestion. The final plasmid was used to transform *S. aureus* Newman using standard procedure.

For the expression of IsdF-3xFLAG, a fragment encompassing *isdF* and its ribosomal binding site was amplified. The 3xFLAG encoding sequence was amplified from pRB474:*mprFdelCysflag*; both fragments were combined by overlap extension PCR and cloned into pRB474 using restriction digestion. The final plasmid was used to transform *S. aureus* Newman.

For the expression of IsdF-mNeongreen, first pCQ11:*mNeongreen* was constructed by restriction digest substitution of *gfp* in pCQ11:*gfp* with *mNeongreen* obtained from pLOM-S-mNeongreen-EC18153 (Julian Hibberd, Addgene plasmid # 137075; http://n2t.net/addgene:137075; RRID: Addgene_137075). pCQ11:*isdF-mNeongreen* was constructed via restriction digest, *isdF* was obtained via PCR from *S. aureus* COL genomic DNA. pCQ11:*isdF-mNeongreen* was transformed into *E. coli* SA08B as shuttle strain for further cloning into *S. aureus* Newman strains.

Oligonucleotides and endonuclease restriction sites are shown in Appendix–Key resources table.

Mutagenesis using phage transduction

S. aureus Newman Δ*spasrtA::Erm*, Δ*spafloA::Erm*, and Δ*spacrtM::Erm* mutants were created using phage transduction (phage Φ11). Transductions of the respective mutations from the Nebraska transposon mutant library into the markerless deletion mutant Newman Δ*spa* were performed according to the standard transduction protocols.

Plasmid construction for BACTH and β-galactosidase assay

S. aureus USA300 LAC WT chromosomal DNA was used as template to amplify *fhuB*, *mntB*, *isdF*, and *fhuC*. The fragments were cloned into the pKT25 and pUT18C vectors (Euromedex) by restriction digestion. A nonsense codon was integrated in the pKT25:*mntB* construct to terminate translation.

To create truncations of IsdF, the topology of IsdF was predicted using the online tool TOPCONS (**Tsirigos et al., 2015**). pKT25:*isdF* was used as a template and primers to truncate the protein after aa131, aa203, aa260, and aa313 were designed. A KpnI restriction site was incorporated into each primer to allow religation of the plasmid after PCR amplification.

For the exchange of alanine position 213 and glycine position 217 to phenylalanines (*isdF_A213F*, *isdF_G217F, isdF_A+G_F*), pKT25:*isdF* was used as PCR template with primers including respective point mutations for the site-directed mutagenesis. The PCR product was digested using DpnI for 3 hr at 37°C, and subsequently, *E. coli* XL-1 blue was transformed with the obtained plasmid.

For the exchange of the coupling helix of MntB to the one from IsdF, *mntB* was amplified from the template pKT25:*mntB* using primers that contained the coupling helix sequence of *isdF* instead of the original sequence via overlap extension PCR. The obtained *mntB_CH*$_{isdF}$ was cloned into the original pKT25:*mntB* plasmid via restriction digest after excising *mntB* from it.

E. coli XL-1 blue was transformed with the different plasmids and the sequence was confirmed by Sanger sequencing.

Oligonucleotides and endonuclease restriction sites are shown in Appendix–Key resources table.

Topology prediction, alignments, and visualization

The topologies of the permeases were predicted using TOPCONS (**Tsirigos et al., 2015**). Additionally, the structure of IsdF was predicted using Alphafold (**Jumper et al., 2021**; **Varadi et al., 2022**) and visualized using PyMOL (The PyMOL Molecular Graphics System, Version 2.5, Schrödinger, LLC). Coupling helixes of permeases were aligned using Clustal Omega.

Purification of hHb

hHb was purified as described elsewhere (**Pishchany et al., 2013**).

Spent media containing SA and SB

SA- and SB-containing spent media were obtained from *S. aureus* USA300 JE2 Δ*sbn* (deletion of SB biosynthesis genes) and Δ*sfa* (deletion of SA biosynthesis genes), respectively. Strains were grown in

BHI with 10 µM of the iron chelator ethylenediamine-*N*,*N*′-bis(2-hydroxyphenylacetic acid) (EDDHA) (LGC Standards) to induce expression of iron-regulated genes for 3 days at 37°C with agitation. The supernatants were collected, sterile filtered, and the obtained spent media were used as SA- or SB-iron source in growth assays.

Growth in iron-limited medium

Staphylococcal deletion mutant strains were grown overnight in TSB at 37°C with agitation. Cells were harvested and washed with RPMI containing 1% CA and 10 µM EDDHA. OD_{600} was adjusted to 1 and 2.5 µl were mixed with 500 µl of RPMI+1% CA+10 µM EDDHA per well (final OD_{600} of 0.005) in a 48-well microtiter plate (Nunc, Thermo Scientific) or 0.5 µl were mixed with 100 µl RPMI+1% CA+10 µM EDDHA per well in a 96-well microtiter plate (Falcon flat bottom, Fisher Scientific), respectively. One µg/ml, 2.5 µg/ml hHb (own purification), 200 ng/ml aerobactin (EMC Microcollections), 200 ng/ml ferrichrome (EMC Microcollections), 5.7% spent medium from USA300 JE2 Δ*sbn* containing SA, 9.1% spent medium from USA300 JE2 Δ*sfa* containing SB, or 20 µM $FeSO_4$ were added as iron sources. 10 µM ZA (Santa Cruz Biotechnology) were used to inhibit membrane microdomain assembly (stock dissolved in 1:1 DMSO:methanol) or as a control the same amount of DMSO/methanol. OD_{600} was measured every 15 min for 24 hr in an Epoch2 reader (BioTek) at 37°C orbital shaking.

BACTH assay

To investigate interactions between the ATPase FhuC and different permeases, the commercially available BACTH kit was used (Euromedex). In brief, *E. coli* BTH101 was co-transformed with the plasmid pKT25 expressing one of the permeases and pUT18C:*fhuC*. The vectors encode for the T25 and T18 catalytic domain of *Bordetella pertussis* adenylate cyclase, respectively. In case of direct interaction of the proteins of interest, these catalytic domains heterodimerize producing cyclic AMP (cAMP) leading to *lacZ* expression. This can be detected as blue colony formation on indicator plates consisting of LB agar 40 µg/ml X-Gal, 0.5 mM isopropyl β-D-1-thiogalactopyranoside (IPTG) (Thermo Scientific), 100 µg/ml ampicillin, and 50 µg/ml kanamycin after 1 day at 30°C. As negative controls, empty vectors were used. As positive control, pKT25:*zip*+pUT18C:*zip* were used encoding a leucine zipper.

β-Galactosidase assay

β-Galactosidase activity was measured to quantify the protein-protein interaction seen in BACTH assay. This activity correlates with the production of cAMP by heterodimerization of T25 and T18 domains. The measurement was performed similarly as described previously (***Griffith and Wolf, 2002***). In brief, *E. coli* BTH101 co-transformed with pKT25 and pUT18C plasmids were inoculated in 800 µl of LB containing 0.5 mM IPTG, 100 µg/ml ampicillin, and 50 µg/ml kanamycin overnight at 37°C with agitation. OD_{600} was measured, and 200 µl of the overnight cultures were mixed with 1 ml of buffer Z (60 mM Na_2HPO_4, 40 mM NaH_2PO_4, 10 mM KCl, 1 mM $MgSO_4$, 50 mM β-mercaptoethanol), 40 µl of 0.1% SDS, and 80 µl of chloroform for 30 min at room temperature to allow permeabilization of cells. One-hundred µl of the aqueous upper phase were transferred to a 96-well microtiter plate, and 20 µl of 4 mg/ml 2-nitrophenyl β-D-galactopyranoside (ONPG) were added to start the calorimetric reaction. OD_{420} and OD_{550} were measured for 4 hr. The highest OD_{420} and its corresponding OD_{550} and t values were used. Blanks were substracted from OD_{600} (blank = LB), OD_{420} and OD_{550} (blank = 100 µl of buffer Z, 0.1% SDS, chloroform, ONPG). The β-galactosidase activity was calculated using the formula $1000*((OD_{420} - 1.75*OD_{550})/(t*v*OD_{600}))$ with t=reaction time in min and v=reaction volume 0.12 ml.

Isolation of cell membranes of *S. aureus*

Strains were grown overnight in RPMI+1% CA at 37°C with agitation. Cells were harvested, resuspendend in 10 ml of PBS buffer with 5 µg/ml DNaseI (from bovine pancreas, Roche) and 10 µg/ml lysostaphin, and incubated for 20 min at 37°C to allow cell lysis. One mM phenylmethylsulfonylfluoride (Roth) was added, and cells were disrupted by adding 5 ml of glass beads using a FastPrep-24 (MP Biomedicals) for two times 40 s 6.5 m/s. Unbroken cells and debris were removed by centrifugation for 10 min 11,000 × *g* at 4°C. The supernatant was ultracentrifuged for 1 hr 100,000 × *g* at 4°C to separate the membrane fraction. The pelleted membrane fraction was dissolved overnight at 4°C for further analysis.

DRM/DSM assay

For separation of cell membranes into DRM and DSM, the CelLytic MEM protein extraction kit (Sigma) was used as described elsewhere (**López and Kolter, 2010**). Cell membranes were isolated as described above and dissolved overnight rotating at 4°C in 600 µl lysis and separation working solution. Equal amounts of DRM and DSM fractions were analyzed by SDS-PAGE followed by Coomassie staining and western blotting for detection of IsdF-3xFLAG using an anti-FLAG M2 antibody (Sigma, #F3165) and infrared imaging (Odyssey CLx, LI-COR). Using Image Studio, IsdF-3xFLAG signals were quantified; with Microsoft Excel and GraphPad Prism 8, DRM and DSM signal intensities were calculated as amount of the total signal (DRM+DSM).

Co-immunoprecipitation

During the co-immunoprecipitation assays, samples were kept at 4°C throughout the experiment. After isolation of cell membranes, 12 mg were dissolved overnight rotating at 4°C in 2 ml of 50 mM Tris HCl pH 8, 250 mM NaCl, 1% *n*-dodecyl-β-D-maltopyranosid (DDM) (Roth). Unsolubilized membrane was removed by centrifugation at 16,200 × *g* 20 min at 4°C. The supernatant was added to a polypropylene column (Bio-Rad) containing 500 µl of profinity IMAC resin Ni-charged (Bio-Rad) and mixed for 30 min rotating at 4°C. The Ni resin slurry was equilibrated with 10 column volumes (CV) of 50 mM Tris HCl pH 8, 250 mM NaCl before. The column was washed with 10 CV of 50 mM Tris HCl pH 8, 250 mM NaCl, 0.04% DDM, and 10 CV of the same buffer with 10 mM imidazole. Bound proteins were eluted with 1 ml of 50 mM Tris HCl pH 8, 250 mM NaCl, 0.04% DMM, 50 mM imidazole. The elution fraction was precipitated with 10% trichloroacetic acid (Merck) and analyzed by western blotting for detection of 3xFLAG-tagged IsdF using an anti-FLAG M2 antibody (Sigma, #F3165) and infrared imaging (Odyssey CLx, LI-COR). Using Image Studio, IsdF-3xFLAG signals were quantified. Using Microsoft Excel and GraphPad Prism 8, IsdF-3xFLAG signals were calculated as ratio between the FloA-His strain and control strain with the control strain set to 1.

Cell fractionation

For separation of bacterial cells into cell wall, membrane, and cytosolic fraction, *S. aureus* Newman strains were grown in RPMI+1% CA overnight. Fractionation was performed as described elsewhere (**Heilbronner et al., 2016**). Cell wall and membrane fractions were analyzed by SDS-PAGE followed by western blotting. IsdA was detected using rabbit serum anti-IsdA and infrared imaging (Odyssey CLx, LI-COR).

Fluorescence microscopy

For fluorescence microscopy of IsdF-mNeongreen and FloA-SNAP, main culture of *S. aureus* Newman *floA-SNAP* pCQ11:*isdF-mNeongreen* (or Newman Δ*floA* pCQ11:*isdF-mNeongreen* and Newman *floA*_R pCQ11:*isdF-mNeongreen* as controls) was inoculated to OD_{600}=0.05 from an overnight culture and grown in MH medium at 37°C under constant shaking for 6 hr. Induction of *isdF-mNeongreen* expression was achieved with 0.1 mM IPTG. FloA-SNAP was labeled with 0.2 µM SNAP-Cell TMR-Star (New England Biolabs, #S9105S) during the last 20 min of main culture incubation. All samples were washed three times in MH medium prior to microscopy. Cells were transferred to a microscopy slide coated with 1% agarose for microscopy. Microscopy was performed on a Carl Zeiss AxioObserver Z1 equipped with a X-Cite Xylis LED Lamp, an αPlan-APOCHROMAT ×100/1.46 oil immersion objective and an AxioCam MRm camera. Visualization IsdF-mNeongreen was achieved using Carl Zeiss filter set 38 (450–490 nm excitation, 495 nm beam splitter, and 500–500 nm emission). Visualization of SNAP-Cell TMR-Star was achieved using Carl Zeiss filter set 43 (538–562 nm excitation, 570 nm beam splitter, and 570–640 nm emission). Deconvolution was achieved using Carl Zeiss Zen 3.6 direct processing. Image analysis was performed using Fiji (ImageJ) Version 2.0.0-rc-69/1.52p; Java 1.8.0_172 (64-bit) (**Schindelin et al., 2012**) and the ImageJ plug-in MicrobeJ 5.13n (9) – beta (**Ducret et al., 2016**). Statistical analysis was performed with GraphPad Prism 8.0.2 (263).

Acknowledgements

The authors thank Prof. J Geoghegan for providing anti-IsdA antiserum and Gina Marke for construction of plasmid pCQ11-IsdF-mNeongreen. The authors thank Libera Lo Presti and Timothy J Foster

for critically reading and editing this manuscript. We acknowledge funding by the German Center of Infection Research (DZIF) TTU 08.708_00 to SH. Additionally, we acknowledge funding by the Deutsche Forschungsgemeinschaft DFG (German Research Foundation) in the frame of Germany´s Excellence Strategy – EXC 2124-390838134 (SH). Further, we acknowledge support by the Fortüne Program of the University Hospital Tübingen 2507-0-0 (SH). Work of DL was supported by Spanish Ministry of Science (PID2020-115699GB-100), and that of FG and SH was funded by the Deutsche Forschungsgemeinschaft (DFG, German Research Foundation) Project-ID 398967434-TRR261. We acknowledge support from the Open Access Publication Fund of the University of Tübingen.

Additional information

Funding

Funder	Grant reference number	Author
German Center of Infection Research	TTU 08.708_00	Simon Heilbronner
Deutsche Forschungsgemeinschaft	EXC 2124 - 390838134	Simon Heilbronner
Fortuene Program University Hospital Tuebingen	2507-0-0	Simon Heilbronner
Spanish Ministry of Science	PID2020-115699GB-100	Daniel Lopez
Deutsche Forschungsgemeinschaft	398967434 -TRR261	Simon Heilbronner

The funders had no role in study design, data collection and interpretation, or the decision to submit the work for publication.

Author contributions

Lea Antje Adolf, Data curation, Investigation, Visualization, Methodology, Writing – original draft; Angelika Müller-Jochim, Lara Kricks, Supervision, Investigation, Methodology; Jan-Samuel Puls, Investigation, Visualization, Methodology; Daniel Lopez, Fabian Grein, Supervision, Methodology, Writing – review and editing; Simon Heilbronner, Conceptualization, Resources, Formal analysis, Supervision, Funding acquisition, Investigation, Visualization, Methodology, Project administration, Writing – review and editing

Author ORCIDs

Jan-Samuel Puls http://orcid.org/0000-0002-8130-7375
Daniel Lopez http://orcid.org/0000-0002-8627-3813
Simon Heilbronner http://orcid.org/0000-0002-6774-2311

Decision letter and Author response

Decision letter https://doi.org/10.7554/eLife.85304.sa1
Author response https://doi.org/10.7554/eLife.85304.sa2

Additional files

Supplementary files

- MDAR checklist

Data availability

All datasets underlying the diagrams are provided as Source Data.

References

Abi-Khalil E, Segond D, Terpstra T, André-Leroux G, Kallassy M, Lereclus D, Bou-Abdallah F, Nielsen-Leroux C. 2015. Heme interplay between ilsa and isdc: two structurally different surface proteins from bacillus cereus. *Biochimica et Biophysica Acta* **1850**:1930–1941. DOI: https://doi.org/10.1016/j.bbagen.2015.06.006, PMID: 26093289

Bach JN, Bramkamp M. 2013. Flotillins functionally organize the bacterial membrane. *Molecular Microbiology* **88**:1205–1217. DOI: https://doi.org/10.1111/mmi.12252, PMID: 23651456

Beasley FC, Vinés ED, Grigg JC, Zheng Q, Liu S, Lajoie GA, Murphy MEP, Heinrichs DE. 2009. Characterization of staphyloferrin a biosynthetic and transport mutants in *Staphylococcus aureus*. *Molecular Microbiology* **72**:947–963. DOI: https://doi.org/10.1111/j.1365-2958.2009.06698.x, PMID: 19400778

Beasley FC, Marolda CL, Cheung J, Buac S, Heinrichs DE. 2011. *Staphylococcus aureus* transporters hts, sir, and sst capture iron liberated from human transferrin by staphyloferrin A, staphyloferrin B, and catecholamine stress hormones, respectively, and contribute to virulence. *Infection and Immunity* **79**:2345–2355. DOI: https://doi.org/10.1128/IAI.00117-11, PMID: 21402762

Beis K. 2015. Structural basis for the mechanism of ABC transporters. *Biochemical Society Transactions* **43**:889–893. DOI: https://doi.org/10.1042/BST20150047, PMID: 26517899

Bramkamp M, Lopez D. 2015. Exploring the existence of lipid rafts in bacteria. *Microbiology and Molecular Biology Reviews* **79**:81–100. DOI: https://doi.org/10.1128/MMBR.00036-14, PMID: 25652542

Brown DA. 2002. Isolation and use of rafts. *Current Protocols in Immunology* **11**:s51. DOI: https://doi.org/10.1002/0471142735.im1110s51, PMID: 18432868

Brückner R. 1992. A series of shuttle vectors for *Bacillus subtilis* and *Escherichia coli*. *Gene* **122**:187–192. DOI: https://doi.org/10.1016/0378-1119(92)90048-t, PMID: 1452028

Cassat JE, Skaar EP. 2013. Iron in infection and immunity. *Cell Host & Microbe* **13**:509–519. DOI: https://doi.org/10.1016/j.chom.2013.04.010, PMID: 23684303

Cheung J, Beasley FC, Liu S, Lajoie GA, Heinrichs DE. 2009. Molecular characterization of staphyloferrin B biosynthesis in *Staphylococcus aureus*. *Molecular Microbiology* **74**:594–608. DOI: https://doi.org/10.1111/j.1365-2958.2009.06880.x, PMID: 19775248

Cotton JL, Tao J, Balibar CJ. 2009. Identification and characterization of the *Staphylococcus aureus* gene cluster coding for staphyloferrin A. *Biochemistry* **48**:1025–1035. DOI: https://doi.org/10.1021/bi801844c, PMID: 19138128

Dassa E, Bouige P. 2001. The ABC of ABCs: a phylogenetic and functional classification of ABC systems in living organisms. *Research in Microbiology* **152**:211–229. DOI: https://doi.org/10.1016/s0923-2508(01)01194-9, PMID: 11421270

Ducret A, Quardokus EM, Brun YV. 2016. MicrobeJ, a tool for high throughput bacterial cell detection and quantitative analysis. *Nature Microbiology* **1**:16077. DOI: https://doi.org/10.1038/nmicrobiol.2016.77, PMID: 27572972

Farnoud AM, Toledo AM, Konopka JB, Del Poeta M, London E. 2015. Raft-like membrane domains in pathogenic microorganisms. *Current Topics in Membranes* **75**:233–268. DOI: https://doi.org/10.1016/bs.ctm.2015.03.005, PMID: 26015285

Ferreira MJ, Sá-Nogueira I de. 2010. A multitask atpase serving different abc-type sugar importers in *Bacillus subtilis*. *Journal of Bacteriology* **192**:5312–5318. DOI: https://doi.org/10.1128/JB.00832-10, PMID: 20693325

Ferreira MJ, Mendes AL, de Sá-Nogueira I. 2017. The msmx atpase plays a crucial role in pectin mobilization by *Bacillus subtilis*. *PLOS ONE* **12**:e0189483. DOI: https://doi.org/10.1371/journal.pone.0189483, PMID: 29240795

Fey PD, Endres JL, Yajjala VK, Widhelm TJ, Boissy RJ, Bose JL, Bayles KW, Bush K. 2013. A genetic resource for rapid and comprehensive phenotype screening of nonessential *Staphylococcus aureus* genes. *MBio* **4**:e00537. DOI: https://doi.org/10.1128/mBio.00537-12, PMID: 23404398

Flannagan RS, Brozyna JR, Kumar B, Adolf LA, Power JJ, Heilbronner S, Heinrichs DE. 2022. In vivo growth of Staphylococcus lugdunensis is facilitated by the concerted function of heme and non-heme iron acquisition mechanisms. *The Journal of Biological Chemistry* **298**:101823. DOI: https://doi.org/10.1016/j.jbc.2022.101823, PMID: 35283192

Foster TJ. 2019. Can β-lactam antibiotics be resurrected to combat MRSA? *Trends in Microbiology* **27**:26–38. DOI: https://doi.org/10.1016/j.tim.2018.06.005

García-Fernández E, Koch G, Wagner RM, Fekete A, Stengel ST, Schneider J, Mielich-Süss B, Geibel S, Markert SM, Stigloher C, Lopez D. 2017. Membrane microdomain disassembly inhibits MRSA antibiotic resistance. *Cell* **171**:1354–1367.. DOI: https://doi.org/10.1016/j.cell.2017.10.012, PMID: 29103614

Gat O, Zaide G, Inbar I, Grosfeld H, Chitlaru T, Levy H, Shafferman A. 2008. Characterization of Bacillus anthracis iron-regulated surface determinant (Isd) proteins containing neat domains. *Molecular Microbiology* **70**:983–999. DOI: https://doi.org/10.1111/j.1365-2958.2008.06460.x, PMID: 18826411

Gill SR, Fouts DE, Archer GL, Mongodin EF, DeBoy RT, Ravel J, Paulsen IT, Kolonay JF, Brinkac L, Beanan M, Dodson RJ, Daugherty SC, Madupu R, Angiuoli SV, Durkin AS, Haft DH, Vamathevan J, Khouri H, Utterback T, Lee C, et al. 2005. Insights on evolution of virulence and resistance from the complete genome analysis of an early methicillin-resistant *Staphylococcus aureus* strain and a biofilm-producing methicillin-resistant Staphylococcus epidermidis strain . *Journal of Bacteriology* **187**:2426–2438. DOI: https://doi.org/10.1128/JB.187.7.2426-2438.2005

Griffith KL, Wolf RE. 2002. Measuring β-galactosidase activity in bacteria: cell growth, permeabilization, and enzyme assays in 96-well arrays. *Biochemical and Biophysical Research Communications* **290**:397–402. DOI: https://doi.org/10.1006/bbrc.2001.6152

Grigg JC, Vermeiren CL, Heinrichs DE, Murphy MEP. 2007. Heme coordination by *Staphylococcus aureus* IsdE. *The Journal of Biological Chemistry* **282**:28815–28822. DOI: https://doi.org/10.1074/jbc.M704602200, PMID: 17666394

Heilbronner S, Holden MTG, van Tonder A, Geoghegan JA, Foster TJ, Parkhill J, Bentley SD. 2011. Genome sequence of staphylococcus lugdunensis n920143 allows identification of putative colonization and virulence factors. *FEMS Microbiology Letters* **322**:60–67. DOI: https://doi.org/10.1111/j.1574-6968.2011.02339.x, PMID: 21682763

Heilbronner S., Hanses F, Monk IR, Speziale P, Foster TJ. 2013. Sortase A promotes virulence in experimental Staphylococcus lugdunensis endocarditis. *Microbiology* **159**:2141–2152. DOI: https://doi.org/10.1099/mic.0.070292-0, PMID: 23943787

Heilbronner S., Monk IR, Brozyna JR, Heinrichs DE, Skaar EP, Peschel A, Foster TJ. 2016. Competing for iron: duplication and amplification of the Isd locus in Staphylococcus lugdunensis HKU09-01 provides a competitive advantage to overcome nutritional limitation. *PLOS Genetics* **12**:e1006246. DOI: https://doi.org/10.1371/journal.pgen.1006246, PMID: 27575058

Hekstra D, Tommassen J. 1993. Functional exchangeability of the ABC proteins of the periplasmic binding protein-dependent transport systems ugp and MAL of *Escherichia coli*. *Journal of Bacteriology* **175**:6546–6552. DOI: https://doi.org/10.1128/jb.175.20.6546-6552.1993, PMID: 8407831

Hollenstein K, Dawson RJP, Locher KP. 2007. Structure and mechanism of ABC transporter proteins. *Current Opinion in Structural Biology* **17**:412–418. DOI: https://doi.org/10.1016/j.sbi.2007.07.003, PMID: 17723295

Hurtubise Y, Shareck F, Kluepfel D, Morosoli R. 1995. A cellulase/xylanase-negative mutant of Streptomyces lividans 1326 defective in cellobiose and xylobiose uptake is mutated in a gene encoding a protein homologous to ATP-binding proteins. *Molecular Microbiology* **17**:367–377. DOI: https://doi.org/10.1111/j.1365-2958.1995.mmi_17020367.x, PMID: 7494485

Jin B, Newton SMC, Shao Y, Jiang X, Charbit A, Klebba PE. 2006. Iron acquisition systems for ferric hydroxamates, haemin and haemoglobin in Listeria monocytogenes. *Molecular Microbiology* **59**:1185–1198. DOI: https://doi.org/10.1111/j.1365-2958.2005.05015.x, PMID: 16430693

Jochim A, Adolf L, Belikova D, Schilling NA, Setyawati I, Chin D, Meyers S, Verhamme P, Heinrichs DE, Slotboom DJ, Heilbronner S. 2020. An ECF-type transporter scavenges heme to overcome iron-limitation in Staphylococcus lugdunensis *eLife* **9**:e57322. DOI: https://doi.org/10.7554/eLife.57322, PMID: 32515736

Jumper J, Evans R, Pritzel A, Green T, Figurnov M, Ronneberger O, Tunyasuvunakool K, Bates R, Žídek A, Potapenko A, Bridgland A, Meyer C, Kohl SAA, Ballard AJ, Cowie A, Romera-Paredes B, Nikolov S, Jain R, Adler J, Back T, et al. 2021. Highly accurate protein structure prediction with alphafold. *Nature* **596**:583–589. DOI: https://doi.org/10.1038/s41586-021-03819-2

Klebba PE, Charbit A, Xiao Q, Jiang X, Newton SM. 2012. Mechanisms of iron and haem transport by Listeria monocytogenes. *Molecular Membrane Biology* **29**:69–86. DOI: https://doi.org/10.3109/09687688.2012.694485, PMID: 22703022

Koch G, Wermser C, Acosta IC, Kricks L, Stengel ST, Yepes A, Lopez D. 2017. Attenuating *Staphylococcus aureus* virulence by targeting flotillin protein scaffold activity. *Cell Chemical Biology* **24**:845–857.. DOI: https://doi.org/10.1016/j.chembiol.2017.05.027, PMID: 28669526

Leisico F, Godinho LM, Gonçalves IC, Silva SP, Carneiro B, Romão MJ, Santos-Silva T, de Sá-Nogueira I. 2020. Multitask ATPases (nbds) of bacterial ABC importers type I and their interspecies exchangeability. *Scientific Reports* **10**:19564. DOI: https://doi.org/10.1038/s41598-020-76444-0, PMID: 33177617

Linke CM, Woodiga SA, Meyers DJ, Buckwalter CM, Salhi HE, King SJ. 2013. The ABC transporter encoded at the pneumococcal fructooligosaccharide utilization locus determines the ability to utilize long- and short-chain fructooligosaccharides. *Journal of Bacteriology* **195**:1031–1041. DOI: https://doi.org/10.1128/JB.01560-12, PMID: 23264576

Liu CI, Jeng WY, Chang WJ, Ko TP, Wang AHJ. 2012. Binding modes of zaragozic acid A to human squalene synthase and staphylococcal dehydrosqualene synthase. *The Journal of Biological Chemistry* **287**:18750–18757. DOI: https://doi.org/10.1074/jbc.M112.351254, PMID: 22474324

Locher KP. 2009. Review structure and mechanism of ATP-binding cassette transporters. *Philosophical Transactions of the Royal Society of London. Series B, Biological Sciences* **364**:239–245. DOI: https://doi.org/10.1098/rstb.2008.0125, PMID: 18957379

López D, Kolter R. 2010. Functional microdomains in bacterial membranes. *Genes & Development* **24**:1893–1902. DOI: https://doi.org/10.1101/gad.1945010, PMID: 20713508

Lopez D, Koch G. 2017. Exploring functional membrane microdomains in bacteria: an overview. *Current Opinion in Microbiology* **36**:76–84. DOI: https://doi.org/10.1016/j.mib.2017.02.001, PMID: 28237903

Lorenz LL, Duthie ES. 1952. Staphylococcal coagulase: mode of action and antigenicity. *Microbiology* **6**:95–107. DOI: https://doi.org/10.1099/00221287-6-1-2-95

Lund VA, Wacnik K, Turner RD, Cotterell BE, Walther CG, Fenn SJ, Grein F, Wollman AJ, Leake MC, Olivier N, Cadby A, Mesnage S, Jones S, Foster SJ. 2018. Molecular coordination of *Staphylococcus aureus* cell division. *eLife* **7**:e32057. DOI: https://doi.org/10.7554/eLife.32057, PMID: 29465397

Madeira F, Pearce M, Tivey ARN, Basutkar P, Lee J, Edbali O, Madhusoodanan N, Kolesnikov A, Lopez R. 2022. Search and sequence analysis tools services from EMBL-EBI in 2022. *Nucleic Acids Research* **50**:W276–W279. DOI: https://doi.org/10.1093/nar/gkac240, PMID: 35412617

Maresso AW, Chapa TJ, Schneewind O. 2006. Surface protein IsdC and sortase B are required for heme-iron scavenging of Bacillus anthracis. *Journal of Bacteriology* **188**:8145–8152. DOI: https://doi.org/10.1128/JB.01011-06, PMID: 17012401

Marion C, Aten AE, Woodiga SA, King SJ. 2011. Identification of an ATPase, msmk, which energizes multiple carbohydrate ABC transporters in Streptococcus pneumoniae. *Infection and Immunity* **79**:4193–4200. DOI: https://doi.org/10.1128/IAI.05290-11, PMID: 21825065

Marraffini LA, Dedent AC, Schneewind O. 2006. Sortases and the art of anchoring proteins to the envelopes of Gram-positive bacteria. *Microbiology and Molecular Biology Reviews* **70**:192–221. DOI: https://doi.org/10.1128/MMBR.70.1.192-221.2006, PMID: 16524923

Matsumoto K, Kusaka J, Nishibori A, Hara H. 2006. Lipid domains in bacterial membranes. *Molecular Microbiology* **61**:1110–1117. DOI: https://doi.org/10.1111/j.1365-2958.2006.05317.x, PMID: 16925550

Mazmanian SK, Ton-That H, Su K, Schneewind O. 2002. An iron-regulated sortase anchors a class of surface protein during *Staphylococcus aureus* pathogenesis. *PNAS* **99**:2293–2298. DOI: https://doi.org/10.1073/pnas.032523999, PMID: 11830639

Mazmanian SK, Skaar EP, Gaspar AH, Humayun M, Gornicki P, Jelenska J, Joachmiak A, Missiakas DM, Schneewind O. 2003. Passage of heme-iron across the envelope of *Staphylococcus aureus*. *Science* **299**:906–909. DOI: https://doi.org/10.1126/science.1081147, PMID: 12574635

Mielich-Süss B, Wagner RM, Mietrach N, Hertlein T, Marincola G, Ohlsen K, Geibel S, Lopez D. 2017. Flotillin scaffold activity contributes to type VII secretion system assembly in *Staphylococcus aureus*. *PLOS Pathogens* **13**:e1006728. DOI: https://doi.org/10.1371/journal.ppat.1006728, PMID: 29166667

Miethke M, Marahiel MA. 2007. Siderophore-based iron acquisition and pathogen control. *Microbiology and Molecular Biology Reviews* **71**:413–451. DOI: https://doi.org/10.1128/MMBR.00012-07, PMID: 17804665

Monk IR, Shah IM, Xu M, Tan MW, Foster TJ. 2012. Transforming the untransformable: application of direct transformation to manipulate genetically *Staphylococcus aureus* and Staphylococcus epidermidis. *MBio* **3**:e00277-11. DOI: https://doi.org/10.1128/mBio.00277-11, PMID: 22434850

Monk IR, Tree JJ, Howden BP, Stinear TP, Foster TJ. 2015. Complete bypass of restriction systems for major *Staphylococcus aureus* lineages. *MBio* **6**: –e00315. DOI: https://doi.org/10.1128/mBio.00308-15, PMID: 26015493

Morabbi Heravi K, Watzlawick H, Altenbuchner J. 2019. The melredca operon encodes a utilization system for the raffinose family of oligosaccharides in *Bacillus subtilis Journal of Bacteriology* **201**:15. DOI: https://doi.org/10.1128/JB.00109-19, PMID: 31138628

Murdoch CC, Skaar EP. 2022. Nutritional immunity: the battle for nutrient metals at the host-pathogen interface. *Nature Reviews. Microbiology* **20**:657–670. DOI: https://doi.org/10.1038/s41579-022-00745-6, PMID: 35641670

Pishchany G, Haley KP, Skaar EP. 2013. *Staphylococcus aureus* growth using human hemoglobin as an iron source. *Journal of Visualized Experiments* **72**:50072. DOI: https://doi.org/10.3791/50072, PMID: 23426144

Quentin Y, Fichant G, Denizot F. 1999. Inventory, assembly and analysis of *Bacillus subtilis* ABC transport systems. *Journal of Molecular Biology* **287**:467–484. DOI: https://doi.org/10.1006/jmbi.1999.2624, PMID: 10092453

Rees DC, Johnson E, Lewinson O. 2009. Abc transporters: the power to change. *Nature Reviews. Molecular Cell Biology* **10**:218–227. DOI: https://doi.org/10.1038/nrm2646, PMID: 19234479

Schaible UE, Kaufmann SHE. 2004. Iron and microbial infection. *Nature Reviews. Microbiology* **2**:946–953. DOI: https://doi.org/10.1038/nrmicro1046, PMID: 15550940

Schindelin J, Arganda-Carreras I, Frise E, Kaynig V, Longair M, Pietzsch T, Preibisch S, Rueden C, Saalfeld S, Schmid B, Tinevez JY, White DJ, Hartenstein V, Eliceiri K, Tomancak P, Cardona A. 2012. Fiji: an open-source platform for biological-image analysis. *Nature Methods* **9**:676–682. DOI: https://doi.org/10.1038/nmeth.2019, PMID: 22743772

Schlösser A. 2000. MsiK-dependent trehalose uptake in Streptomyces reticuli. *FEMS Microbiology Letters* **184**:187–192. DOI: https://doi.org/10.1111/j.1574-6968.2000.tb09012.x, PMID: 10713419

Schönert S, Seitz S, Krafft H, Feuerbaum EA, Andernach I, Witz G, Dahl MK. 2006. Maltose and maltodextrin utilization by *Bacillus subtilis*. *Journal of Bacteriology* **188**:3911–3922. DOI: https://doi.org/10.1128/JB.00213-06, PMID: 16707683

Sebulsky MT, Hohnstein D, Hunter MD, Heinrichs DE. 2000. Identification and characterization of a membrane permease involved in iron-hydroxamate transport in *Staphylococcus aureus*. *Journal of Bacteriology* **182**:4394–4400. DOI: https://doi.org/10.1128/JB.182.16.4394-4400.2000, PMID: 10913070

Sebulsky MT, Heinrichs DE. 2001. Identification and characterization of fhud1 and FhuD2, two genes involved in iron-hydroxamate uptake in *Staphylococcus aureus*. *Journal of Bacteriology* **183**:4994–5000. DOI: https://doi.org/10.1128/JB.183.17.4994-5000.2001, PMID: 11489851

Shah MB, Sehgal PB. 2007. Nondetergent isolation of rafts. *Methods in Molecular Biology* **398**:21–28. DOI: https://doi.org/10.1007/978-1-59745-513-8_3, PMID: 18214371

Sheldon JR, Heinrichs DE. 2015. Recent developments in understanding the iron acquisition strategies of gram positive pathogens. *FEMS Microbiology Reviews* **39**:592–630. DOI: https://doi.org/10.1093/femsre/fuv009, PMID: 25862688

Sheldon JR, Laakso HA, Heinrichs DE. 2016. Iron acquisition strategies of bacterial pathogens. *Microbiology Spectrum* **4**:e15. DOI: https://doi.org/10.1128/microbiolspec.VMBF-0010-2015, PMID: 27227297

Skaar EP, Humayun M, Bae T, DeBord KL, Schneewind O. 2004. Iron-source preference of *Staphylococcus aureus* infections. *Science* **305**:1626–1628. DOI: https://doi.org/10.1126/science.1099930, PMID: 15361626

Skaar EP, Gaspar AH, Schneewind O. 2006. Bacillus anthracis IsdG, a heme-degrading monooxygenase. *Journal of Bacteriology* **188**:1071–1080. DOI: https://doi.org/10.1128/JB.188.3.1071-1080.2006, PMID: 16428411

Slavetinsky CJ, Hauser JN, Gekeler C, Slavetinsky J, Geyer A, Kraus A, Heilingbrunner D, Wagner S, Tesar M, Krismer B, Kuhn S, Ernst CM, Peschel A. 2022. Sensitizing *Staphylococcus aureus* to antibacterial agents by decoding and blocking the lipid flippase MprF. *eLife* **11**:e66376. DOI: https://doi.org/10.7554/eLife.66376, PMID: 35044295

Somani VK, Aggarwal S, Singh D, Prasad T, Bhatnagar R. 2016. Identification of novel raft marker protein, flotp in Bacillus anthracis. *Frontiers in Microbiology* **7**:169. DOI: https://doi.org/10.3389/fmicb.2016.00169, PMID: 26925042

Spaan AN, Reyes-Robles T, Badiou C, Cochet S, Boguslawski KM, Yoong P, Day CJ, de Haas CJC, van Kessel KPM, Vandenesch F, Jennings MP, Le Van Kim C, Colin Y, van Strijp JAG, Henry T, Torres VJ. 2015. *Staphylococcus aureus* targets the Duffy antigen receptor for chemokines (DARC) to lysE erythrocytes. *Cell Host & Microbe* **18**:363–370. DOI: https://doi.org/10.1016/j.chom.2015.08.001, PMID: 26320997

Speziali CD, Dale SE, Henderson JA, Vinés ED, Heinrichs DE. 2006. Requirement of *Staphylococcus aureus* ATP-binding cassette-atpase fhuc for iron-restricted growth and evidence that it functions with more than one iron transporter. *Journal of Bacteriology* **188**:2048–2055. DOI: https://doi.org/10.1128/JB.188.6.2048-2055.2006, PMID: 16513734

Sun Z, Zhou D, Zhang X, Li Q, Lin H, Lu W, Liu H, Lu J, Lin X, Li K, Xu T, Bao Q, Zhang H. 2020. Determining the genetic characteristics of resistance and virulence of the `` epidermidis cluster group'' through pan-genome analysis. *Frontiers in Cellular and Infection Microbiology* **10**:274. DOI: https://doi.org/10.3389/fcimb.2020.00274, PMID: 32596166

Tan MF, Gao T, Liu WQ, Zhang CY, Yang X, Zhu JW, Teng MY, Li L, Zhou R. 2015. MsmK, an atpase, contributes to utilization of multiple carbohydrates and host colonization of streptococcus suis. *PLOS ONE* **10**:e0130792. DOI: https://doi.org/10.1371/journal.pone.0130792, PMID: 26222651

ter Beek J, Guskov A, Slotboom DJ. 2014. Structural diversity of ABC transporters. *The Journal of General Physiology* **143**:419–435. DOI: https://doi.org/10.1085/jgp.201411164, PMID: 24638992

Tsirigos KD, Peters C, Shu N, Käll L, Elofsson A. 2015. The TOPCONS web server for consensus prediction of membrane protein topology and signal peptides. *Nucleic Acids Research* **43**:W401–W407. DOI: https://doi.org/10.1093/nar/gkv485, PMID: 25969446

Varadi M, Anyango S, Deshpande M, Nair S, Natassia C, Yordanova G, Yuan D, Stroe O, Wood G, Laydon A, Žídek A, Green T, Tunyasuvunakool K, Petersen S, Jumper J, Clancy E, Green R, Vora A, Lutfi M, Figurnov M, et al. 2022. AlphaFold protein structure database: massively expanding the structural coverage of protein-sequence space with high-accuracy models. *Nucleic Acids Research* **50**:D439–D444. DOI: https://doi.org/10.1093/nar/gkab1061, PMID: 34791371

Webb AJ, Homer KA, Hosie AHF. 2008. Two closely related ABC transporters in streptococcus mutans are involved in disaccharide and/or oligosaccharide uptake. *Journal of Bacteriology* **190**:168–178. DOI: https://doi.org/10.1128/JB.01509-07, PMID: 17965163

Weinberg ED. 1975. Nutritional immunity host's attempt to withold iron from microbial invaders. *JAMA* **231**:39–41. DOI: https://doi.org/10.1001/jama.231.1.39, PMID: 1243565

Wen PC, Tajkhorshid E. 2011. Conformational coupling of the nucleotide-binding and the transmembrane domains in ABC transporters. *Biophysical Journal* **101**:680–690. DOI: https://doi.org/10.1016/j.bpj.2011.06.031, PMID: 21806936

Wieland B, Feil C, Gloria-Maercker E, Thumm G, Lechner M, Bravo JM, Poralla K, Götz F. 1994. Genetic and biochemical analyses of the biosynthesis of the yellow carotenoid 4,4'-diaponeurosporene of *Staphylococcus aureus*. *Journal of Bacteriology* **176**:7719–7726. DOI: https://doi.org/10.1128/jb.176.24.7719-7726.1994, PMID: 8002598

Xiao Q, Jiang X, Moore KJ, Shao Y, Pi H, Dubail I, Charbit A, Newton SM, Klebba PE. 2011. Sortase independent and dependent systems for acquisition of haem and haemoglobin in Listeria monocytogenes. *Molecular Microbiology* **80**:1581–1597. DOI: https://doi.org/10.1111/j.1365-2958.2011.07667.x, PMID: 21545655

Yokoyama H, Matsui I. 2020. The lipid raft markers stomatin, prohibitin, flotillin, and hflk/C (SPFH) -domain proteins form an operon with nfed proteins and function with apolar polyisoprenoid lipids. *Critical Reviews in Microbiology* **46**:38–48. DOI: https://doi.org/10.1080/1040841X.2020.1716682, PMID: 31983249

Zapotoczna M, Heilbronner S, Speziale P, Foster TJ. 2012. Iron-regulated surface determinant (isd) proteins of staphylococcus lugdunensis. *Journal of Bacteriology* **194**:6453–6467. DOI: https://doi.org/10.1128/JB.01195-12, PMID: 23002220

Zolnerciks JK, Andress EJ, Nicolaou M, Linton KJ. 2011. Structure of ABC transporters. *Essays in Biochemistry* **50**:43–61. DOI: https://doi.org/10.1042/bse0500043, PMID: 21967051

Appendix 1

Appendix 1—key resources table

Reagent type (species) or resource	Designation	Source or reference	Identifiers	Additional information
Strain, strain background (*Escherichia coli*)	BTH101	BACTH System (Euromedex)		Used for BACTH assay; F-, *cya-99*, *araD139*, *galE15*, *galK16*, *rpsL1* (Str r), *hsdR2*, *mcrA1*, *mcrB1*
Strain, strain background (*Escherichia coli*)	BTH101 pKT25+pUT18C	This study		BACTH assay
Strain, strain background (*Escherichia coli*)	BTH101 pKT25:*zip*+pUT18C:*zip*	This study		BACTH assay
Strain, strain background (*Escherichia coli*)	BTH101 pKT25:*fhuB*+pUT18C:*fhuC*	This study		BACTH assay
Strain, strain background (*Escherichia coli*)	BTH101 pKT25:*mntB*+pUT18C:*fhuC*	This study		BACTH assay
Strain, strain background (*Escherichia coli*)	BTH101 pKT25:*isdF*+pUT18C:*fhuC*	This study		BACTH assay
Strain, strain background (*Escherichia coli*)	BTH101 pKT25:*isdF_A213F*+pUT18C:*fhuC*	This study		BACTH assay
Strain, strain background (*Escherichia coli*)	BTH101 pKT25:*isdF_G217F*+pUT18C:*fhuC*	This study		BACTH assay
Strain, strain background (*Escherichia coli*)	BTH101 pKT25:*isdF_A+G_F*+pUT18C:*fhuC*	This study		BACTH assay
Strain, strain background (*Escherichia coli*)	BTH101 pKT25:*mntB_CH*$_{isdF}$ +pU18C:*fhuC*	This study		BACTH assay
Strain, strain background (*Escherichia coli*)	BTH101 pKT25:*isdF_short_1*+pUT18C:*fhuC*	This study		BACTH assay
Strain, strain background (*Escherichia coli*)	BTH101 pKT25:*isdF_short_2*+pUT18C:*fhuC*	This study		BACTH assay
Strain, strain background (*Escherichia coli*)	BTH101 pKT25:*isdF_short_3*+pUT18C:*fhuC*	This study		BACTH assay
Strain, strain background (*Escherichia coli*)	BTH101 pKT25:*isdF_short_4*+pUT18C:*fhuC*	This study		BACTH assay
Strain, strain background (*Escherichia coli*)	SA08B	**Monk et al., 2015**		Used for cloning of pIMAY, pRB474 and pRB473 plasmids; DC10BΩP$_{help}$- *hsdMS* (CC8-2) (SAUSA300_1751) of NRS384 integrated between the *atpI* and *gidB* genes

Appendix 1—key resources table continued on next page

Appendix 1—key resources table continued

Reagent type (species) or resource	Designation	Source or reference	Identifiers	Additional information
Strain, strain background (*Escherichia coli*)	SL01B	**Heilbronner et al., 2013**		Used for cloning of pIMAY for transformations of *S. lugdunensis*; DC10B hsdMS$^+$ (*S. lugdunensis* N920143 (CC1))
Strain, strain background (*Staphylococcus aureus*)	USA300 JE2	**Fey et al., 2013**		WT
Strain, strain background (*Staphylococcus aureus*)	USA300 JE2 Δ*sbn*	This study		Markerless deletion of the entire *sbn* locus (staphyloferrin B biosynthesis genes; *sbnA-I*)
Strain, strain background (*Staphylococcus aureus*)	USA300 JE2 Δ*sfa*	This study		Markerless deletion of the entire *sfa* locus (staphyloferrin A biosynthesis genes; *sfaA-D*)
Strain, strain background (*Staphylococcus aureus*)	USA300 JE2 fhuC::Erm	**Fey et al., 2013**		Nebraska transposon library mutant Δ*fhuC* (SAUSA300_0633)
Strain, strain background (*Staphylococcus aureus*)	USA300 JE2 *floA::Erm*	**Fey et al., 2013**		Nebraska transposon library mutant Δ*floA* (SAUSA300_1533)
Strain, strain background (*Staphylococcus aureus*)	USA300 JE2 *floA*_R	This study		Genomic complementation of the Nebraska transposon library mutant *floA::Erm* with *floA*
Strain, strain background (*Staphylococcus aureus*)	COL	**Gill et al., 2005**		WT
Strain, strain background (*Staphylococcus aureus*)	Newman	**Lorenz and Duthie, 1952**		WT
Strain, strain background (*Staphylococcus aureus*)	Newman Δ*isd*	This study		Markerless deletion mutant of the entire *isd* locus
Strain, strain background (*Staphylococcus aureus*)	Newman Δ*fhu*	This study		Markerless deletion mutant of the entire *fhu* (*fhuCBG*) locus
Strain, strain background (*Staphylococcus aureus*)	Newman Δ*hts*	This study		Markerless deletion mutant of the entire *hts* (*htsABC*) locus
Strain, strain background (*Staphylococcus aureus*)	Newman Δ*sir*	This study		Markerless deletion mutant of the entire *sir* (*sirABC*) locus
Strain, strain background (*Staphylococcus aureus*)	Newman Δ*fhuC*	This study		Markerless deletion mutant of *fhuC*
Strain, strain background (*Staphylococcus aureus*)	Newman Δ*floA*	This study		Markerless deletion mutant of *floA*

Appendix 1—key resources table continued on next page

Appendix 1—key resources table continued

Reagent type (species) or resource	Designation	Source or reference	Identifiers	Additional information
Strain, strain background (*Staphylococcus aureus*)	Newman Δ*crtM*	**Wieland et al., 1994**		Deletion mutant of *crtM* by insertion of Cm resistance gene
Strain, strain background (*Staphylococcus aureus*)	Newman WT pRB473	This study		Empty vector control
Strain, strain background (*Staphylococcus aureus*)	Newman Δ*fhuC* pRB473	This study		Empty vector control
Strain, strain background (*Staphylococcus aureus*)	Newman Δ*fhuC* pRB473:*fhuC*	This study		Expression plasmid for *fhuC* under its native promotor
Strain, strain background (*Staphylococcus aureus*)	Newman Δ*spa*	This study		Markerless deletion mutant of *spa*
Strain, strain background (*Staphylococcus aureus*)	Newman Δ*spa srtA::Erm*	This study		Phage transduction from the Nebraska transposon library mutant *srtA::Erm* (SAUSA300_2467) into Newman Δ*spa*
Strain, strain background (*Staphylococcus aureus*)	Newman Δ*spa floA::Erm*	This study		Phage transduction from the Nebraska transposon library mutant *floA::Erm* (SAUSA300_1533) into Newman Δ*spa*
Strain, strain background (*Staphylococcus aureus*)	Newman Δ*spa crtM::Erm*	This study		Phage transduction from the Nebraska transposon library mutant *crtM::Erm* (SAUSA300_2499) into Newman Δ*spa*
Strain, strain background (*Staphylococcus aureus*)	Newman WT pRB474:*isdF-3xFLAG*	This study		Expression plasmid for *isdF-3xFLAG*
Strain, strain background (*Staphylococcus aureus*)	Newman *floA-6xHis* pRB474:*isdF-3xFLAG*	This study		Insertion of linker+6xHis-tag C-terminally of *floA*; expression plasmid for *isdF-3xFLAG*
Strain, strain background (*Staphylococcus aureus*)	Newman *floA-SNAP* pCQ11:*isdF-mNeongreen*	This study		Insertion of SNAP tag C-terminally of *floA*; expression plasmid for *isdF-mNeongreen*
Strain, strain background (*Staphylococcus aureus*)	Newman Δ*floA* pCQ11:*isdF-mNeongreen*	This study		Markerless deletion of *floA*; expression plasmid for *isdF-mNeongreen*
Strain, strain background (*Staphylococcus aureus*)	Newman *floA*_R pCQ11:*isdF-mNeongreen*	This study		Genomic complementation of the Δ*floA* mutant; expression plasmid for *isdF-mNeongreen*
Strain, strain background (*Staphylococcus lugdunensis*)	N920143	**Heilbronner et al., 2011**		WT
Strain, strain background (*Staphylococcus lugdunensis*)	N920143 Δ*isd*	**Zapotoczna et al., 2012**		Markerless deletion mutant of the entire *isd* locus

Appendix 1—key resources table continued on next page

Appendix 1—key resources table continued

Reagent type (species) or resource	Designation	Source or reference	Identifiers	Additional information
Strain, strain background (*Staphylococcus lugdunensis*)	N920143 Δ*lha*	**Jochim et al., 2020**		Markerless deletion mutant of *lhaSTA*
Strain, strain background (*Staphylococcus lugdunensis*)	N920143 Δ*lha*Δ*floA*	This study		Markerless deletion mutant of *lhaSTA* and *floA*
Biological sample (*Human*)	Human hemoglobin	Own purification (see Materials and methods)		Sex male
Antibody	Mouse monoclonal anti-FLAG M2	Sigma	F3165	WB (1:10,000)
Antibody	Polyclonal IRDye 800CW goat anti-mouse IgG secondary antibody	LI-COR	926-32210	WB (1:10,000)
Antibody	Polyclonal rabbit serum anti-IsdA	Prof. J. Geoghegan		WB (1:5000)
Antibody	Polyclonal IRDye 680RD goat anti-rabbit IgG secondary antibody	LI-COR	926-68071	WB (1:10,000)
Recombinant DNA reagent	pIMAY (plasmid)	**Monk et al., 2012**		*E. coli*/*Staphylococcus* thermo-sensitive vector for allelic replacement in *S. aureus*
Recombinant DNA reagent	pIMAY:Δ*sbn*	This study		Plasmid for the deletion of the entire *sbn* locus
Recombinant DNA reagent	pIMAY:Δ*sfa*	This study		Plasmid for the deletion of the entire *sfa* locus
Recombinant DNA reagent	pIMAY:Δ*floA* complementation	This study		Plasmid for the genomic reversion of in USA300 JE2 *floA*::*Erm* and Newman Δ*floA*
Recombinant DNA reagent	pIMAY:Δ*isd*	This study		Plasmid for the deletion of the entire *isd* locus
Recombinant DNA reagent	pIMAY:Δ*fhu*	This study		Plasmid for the deletion of the entire *fhu* locus
Recombinant DNA reagent	pIMAY:Δ*hts*	This study		Plasmid for the deletion of the entire *hts* locus
Recombinant DNA reagent	pIMAY:Δ*sir*	This study		Plasmid for the deletion of the entire *sir* locus
Recombinant DNA reagent	pIMAY:Δ*fhuC*	This study		Plasmid for the deletion of *fhuC*

Appendix 1—key resources table continued on next page

Appendix 1—key resources table continued

Reagent type (species) or resource	Designation	Source or reference	Identifiers	Additional information
Recombinant DNA reagent	pIMAY:Δ*floA*	This study		Plasmid for the deletion of *floA*
Recombinant DNA reagent	pIMAY:Δ*spa*	This study		Plasmid for the deletion of *spa*
Recombinant DNA reagent	pIMAY:Δ*floA*	This study		Plasmid for the deletion of *floA* in *S. lugdunensis* N920143
Recombinant DNA reagent	pIMAY:*floA-6xHis*	This study		Plasmid for the addition of 6xHis C-terminally to *floA*
Recombinant DNA reagent	pIMAY:*floA-SNAP*	This study		Plasmid for the addition of SNAP C-terminally to *floA*
Recombinant DNA reagent	pRB473 (plasmid)	**Brückner, 1992**		Expression plasmid without a promotor
Recombinant DNA reagent	pRB473:*fhuC*	This study		fhuC expressing plasmid under its native promotor (fur box)
Recombinant DNA reagent	pRB474 (plasmid)	**Brückner, 1992**		Expression plasmid with constitutive promotor
Recombinant DNA reagent	pRB474:*isdF-3xFLAG*	This study		*isdF-3xFLAG* expressing plasmid
Recombinant DNA reagent	pCQ11:*snap*	**Lund et al., 2018**		Used as template for SNAP amplification PCR
Recombinant DNA reagent	pCQ11:*gfp*	C.Quiblier and B. Berger-Bächi		Backbone for pCQ11:*mNeongreen*
Recombinant DNA reagent	pCQ11:*mNeongreen*	This study		Backbone for pCQ11 :*isdF-mNeongreen*
Recombinant DNA reagent	pLOM-S-mNeongreen-EC18153	Addgene plasmid	# 137075	*mNeongreen* template
Recombinant DNA reagent	pCQ11:*isdF-mNeongreen*	This study		*isdF* with C-terminal *mNeongreen* fusion; IPTG inducible
Recombinant DNA reagent	pKT25 (plasmid)	BACTH System (Euromedex)		BACTH assay plasmid, N-terminal T25 fragment
Recombinant DNA reagent	pKT25:*fhuB*	This study		T25 fragment N-terminally of *fhuB*
Recombinant DNA reagent	pKT25:*isdF*	This study		T25 fragment N-terminally of *isdF*
Recombinant DNA reagent	pKT25:*mntB*	This study		T25 fragment N-terminally of *mntB*

Appendix 1—key resources table continued on next page

Appendix 1—key resources table continued

Reagent type (species) or resource	Designation	Source or reference	Identifiers	Additional information
Recombinant DNA reagent	pKT25:*zip*	BACTH System (Euromedex)		T25 fragment N-terminally of *zip*; positive control
Recombinant DNA reagent	pKT25:*isdF_short1*	This study		T25 fragment N-terminally of *isdF_short1*: truncated C-terminus
Recombinant DNA reagent	pKT25:*isdF_short2*	This study		T25 fragment N-terminally of *isdF_short2*: truncated C-terminus+fourth cytosolic loop
Recombinant DNA reagent	pKT25:*isdF_short3*	This study		T25 fragment N-terminally of *isdF_short3*: truncated C-terminus+third cytosolic loop
Recombinant DNA reagent	pKT25:*isdF_short4*	This study		T25 fragment N-terminally of *isdF_short4*: truncated C-terminus+second cytosolic loop
Recombinant DNA reagent	pKT25:*isdF_A213F*	This study		T25 fragment N-terminally of *isdF*: alanine position 213 exchanged to phenylalanine
Recombinant DNA reagent	pKT25:*isdF_G217F*	This study		T25 fragment N-terminally of *isdF*: glycine position 217 exchanged to phenylalanine
Recombinant DNA reagent	pKT25:*isdF_A+G_F*	This study		T25 fragment N-terminally of *isdF*: alanine (213)+glycine (217) exchanged to phenylalanines
Recombinant DNA reagent	pKT25:*mntB_CHisdF*	This study		T25 fragment N-terminally of *mntB*; coupling helix of *mntB* exchanged to the one from *isdF*
Recombinant DNA reagent	pUT18C	BACTH System (Euromedex)		BACTH assay plasmid, N-terminal T18 fragment
Recombinant DNA reagent	pUT18C:*fhuC*	This study		T18 fragment N-terminally of *fhuC*
Recombinant DNA reagent	pUT18C:*zip*	BACTH System (Euromedex)		T18 fragment N-terminally of *zip*; positive control
Recombinant DNA reagent	pRB474:*mprFdelCysflag*	***Slavetinsky et al., 2022***		Used as template for 3xFLAG amplification PCR
Sequence-based reagent	Δsbn_PF-A_SmaI	This study	PCR primer	Primer for Δ*sbnA-I* fragment using pIMAY; CACCTAAAGATCCCGGGACGTCAGTGGC
Sequence-based reagent	Δsbn_PR-B	This study	PCR primer	Primer for Δ*sbnA-I* fragment using pIMAY; CATAGGTGTTTGCCCTACAGAATCTAAC
Sequence-based reagent	Δsbn_PF-C	This study	PCR primer	Primer for Δ*sbnA-I* fragment using pIMAY; CTGTAGGGCAAACACCTATGTAGTTTT ACTGTGATGTTGAGGGAAATA

Appendix 1—key resources table continued on next page

Appendix 1—key resources table continued

Reagent type (species) or resource	Designation	Source or reference	Identifiers	Additional information
Sequence-based reagent	Δsbn_PR-D_KpnI	This study	PCR primer	Primer for Δ*sbnA-I* fragment using pIMAY; AAATCAGCAAGGTACCACCAATCAGCC
Sequence-based reagent	ΔsfaDABC_PF-A_KpnI	This study	PCR primer	Primer for Δ*sfaDABC* fragment using pIMAY; GATCGGTACCAGTATCTTTAGTTGATGATTCT
Sequence-based reagent	ΔsfaDABC_PR-B	This study	PCR primer	Primer for Δ*sfaDABC* fragment using pIMAY; TAATATATTTATCAATAAGTCTAAGTTGACA
Sequence-based reagent	ΔsfaDABC_PF-C	This study	PCR primer	Primer for Δ*sfaDABC* fragment using pIMAY; ACTTATTGATAAATATATTATAAGGT TATAGAATTTTATTAATCGT
Sequence-based reagent	ΔsfaDABC_PR-D	This study	PCR primer	Primer for Δ*sfaDABC* fragment using pIMAY; CGGAATTCTTCTATTGGTAGTGTAAGTTGGATCA
Sequence-based reagent	ΔfloA_PF-A_SacI	This study	PCR primer	Primer for *floA::Erm* and Δ*floA* complementation fragment using pIMAY (*floA*_R); CCAAGGAGCTCTCAATATGCATTCTATC
Sequence-based reagent	ΔfloA comp._PR-B_SmaI	This study	PCR primer	Primer for *floA::Erm* and Δ*floA* complementation fragment using pIMAY (*floA*_R); CTTCACCAACCCGGGCGATGATTGTTTC
Sequence-based reagent	ΔfloA comp._PF-C_SmaI	This study	PCR primer	Primer for *floA::Erm* and Δ*floA* complementation fragment using pIMAY (*floA*_R); GAAACAATCATCGCCCGGGTTGGTGAAG
Sequence-based reagent	ΔfloA_PR-D_KpnI	This study	PCR primer	Primer for *floA::Erm* and Δ*floA* complementation fragment using pIMAY (*floA*_R); TTTTCGGTACCAATGTCAGTACGAATC
Sequence-based reagent	Δisd_PF-A_KpnI	This study	PCR primer	Primer for Δ*isdB-G* fragment using pIMAY; TAAAGGGAACAAAAGCTGGGTACCAT GCAGAGGACTTACTTGCGTAAAG
Sequence-based reagent	Δisd_PR-B	This study	PCR primer	Primer for Δ*isdB-G* fragment using pIMAY; TAAATTAACAAATTTTAATTGGCGGATG
Sequence-based reagent	Δisd_PF-C	This study	PCR primer	Primer for Δ*isdB-G* fragment using pIMAY; ATTAAAATTTGTTAATTTAAGAATTTAAA GAGGTTGCAGTACTTGTTATG
Sequence-based reagent	Δisd_PR-D_SacI	This study	PCR primer	Primer for Δ*isdB-G* fragment using pIMAY; CGACTCACTATAGGGCGAATTGGAGCTC TCAATTAAATGCACACCTTCAATTAAAGC

Appendix 1—key resources table continued on next page

Appendix 1—key resources table continued

Reagent type (species) or resource	Designation	Source or reference	Identifiers	Additional information
Sequence-based reagent	Δfhu_PF-A_SacI	This study	PCR primer	Primer for Δ*fhuCBG* fragment using pIMAY; AATACCTCGAGCTCAGCACGCCATATG CTTTGCTTTTCTTCGAT
Sequence-based reagent	Δfhu_PR-B	This study	PCR primer	Primer for Δ*fhuCBG* fragment using pIMAY; CATAATTTCCCTACTTTCAATAAAATTCTT
Sequence-based reagent	Δfhu_PF-C	This study	PCR primer	Primer for Δ*fhuCBG* fragment using pIMAY; ATTTTATTGAAAGTAGGGAAATTATG TAGTGTCAATGGACACAACTTATTGCTATG
Sequence-based reagent	Δfhu_PR-D_KpnI	This study	PCR primer	Primer for Δ*fhuCBG* fragment using pIMAY; TGCTTTggTAccCTTCTAATATTTTATCAGGTGTAGG
Sequence-based reagent	Δhts_PF-A_SacI	This study	PCR primer	Primer for Δ*htsABC* fragment using pIMAY; GCACgagCTCATTCGATGTATATGAAAAATTTAC
Sequence-based reagent	Δhts_PR-B	This study	PCR primer	Primer for Δ*htsABC* fragment using pIMAY; CATCGTTCCACTCCTTAATATGTATAAC
Sequence-based reagent	Δhts_PF-C	This study	PCR primer	Primer for Δ*htsABC* fragment using pIMAY; TATACATATTAAGGAGTGGAACGATGTA ACTAACATATGATTAGAGTTTAAAAAAG
Sequence-based reagent	Δhts_PR-D_KpnI	This study	PCR primer	Primer for Δ*htsABC* fragment using pIMAY; GTCAGGTacCAATTTATCTTTTAAAATAG
Sequence-based reagent	Δsir_PF-A_SacI	This study	PCR primer	Primer for Δ*sirABC* fragment using pIMAY; GTTTTgAgCtCTTGATTTTAGCTATCATTG
Sequence-based reagent	Δsir_PR-B	This study	PCR primer	Primer for Δ*sirABC* fragment using pIMAY; CATTGACTAATTAGCCTCCTTCGTG
Sequence-based reagent	Δsir_PF-C	This study	PCR primer	Primer for Δ*sirABC* fragment using pIMAY; AGGAGGCTAATTAGTCAATGTAACG ATATTATTAAAACAAAATG
Sequence-based reagent	Δsir_PR-D_KpnI	This study	PCR primer	Primer for Δ*sirABC* fragment using pIMAY; CTGATGgtAccAATAAGTCAGTAATATAAATTC
Sequence-based reagent	PF-A_ΔfhuC_SacI	This study	PCR primer	Primer for Δ*fhuC* fragment using pIMAY; AATACCTCGAGCTCAGCACGCCATAT GCTTTGCTTTTCTTCGAT
Sequence-based reagent	PR-B_ΔfhuC	This study	PCR primer	Primer for Δ*fhuC* fragment using pIMAY; CATAATTTCCCTACTTTCAATAAAATTCTT

Appendix 1—key resources table continued on next page

Appendix 1—key resources table continued

Reagent type (species) or resource	Designation	Source or reference	Identifiers	Additional information
Sequence-based reagent	PF-C_ΔfhuC	This study	PCR primer	Primer for Δ*fhuC* fragment using pIMAY; TTATTGAAAGTAGGGAAATTAT GTAATTAAGTAAGTTAATAT
Sequence-based reagent	PR-D_ΔfhuC_KpnI	This study	PCR primer	Primer for Δ*fhuC* fragment using pIMAY; ATGGTAAGTTGGGTACCCAATTGTTAA TATAATGAATAACGCAATACCA
Sequence-based reagent	ΔfloA_PF-A_SacI	This study	PCR primer	Primer for Δ*floA* fragment using pIMAY; CCAAGGAGCTCTCAATATGCATTCTATC
Sequence-based reagent	ΔfloA_PR-B	This study	PCR primer	Primer for Δ*floA* fragment using pIMAY; AAACATGGTATCGCTCCTTTTAATTAATC
Sequence-based reagent	ΔfloA_PF-C	This study	PCR primer	Primer for Δ*floA* fragment using pIMAY; AAAGGAGCGATACCATGTTTTAAGT CGAGAGGTGATTAAATG
Sequence-based reagent	ΔfloA_PR-D_KpnI	This study	PCR primer	Primer for Δ*floA* fragment using pIMAY; TTTTCGGTACCAATGTCAGTACGAATC
Sequence-based reagent	Δspa_PF-A_SacI	This study	PCR primer	Primer for Δ*spa* fragment using pIMAY; GAAAGAGCTCTTTTAATTCATATGGATGAC
Sequence-based reagent	Δspa_PR-B	This study	PCR primer	Primer for Δ*spa* fragment using pIMAY; CATAATATAACGAATTATGTATTGCAATAC
Sequence-based reagent	Δspa_PF-C	This study	PCR primer	Primer for Δ*spa* fragment using pIMAY; ACATAATTCGTTATATTATGTAAAAAC AAACAATACACAACGATAG
Sequence-based reagent	Δspa_PR-D_KpnI	This study	PCR primer	Primer for Δ*spa* fragment using pIMAY; CAGGTGGGGTACCAGCGAAACTTATTTCAC
Sequence-based reagent	N9_PF-A_ΔfloA_SacI	This study	PCR primer	Primer for Δ*floA* (for *S. lugdunensis* N920143) fragment using pIMAY; CTTTATTGGAGCTCCAGTAATAGGCTTTTTTGGCATAG
Sequence-based reagent	N9_PR-B_ΔfloA	This study	PCR primer	Primer for Δ*floA* (for *S. lugdunensis* N920143) fragment using pIMAY; CATTAAATCACTCCTATAAATTAATCTATC
Sequence-based reagent	N9_PF-C_ΔfloA	This study	PCR primer	Primer for Δ*floA* (for *S. lugdunensis* N920143) fragment using pIMAY; TTTATAGGAGTGATTTAATGTAATTA AAGGGGTGATGTCATGAAC

Appendix 1—key resources table continued on next page

Appendix 1—key resources table continued

Reagent type (species) or resource	Designation	Source or reference	Identifiers	Additional information
Sequence-based reagent	N9_PR-D_ΔfloA_KpnI	This study	PCR primer	Primer for Δ*floA* (for *S. lugdunensis* N920143) fragment using pIMAY; CGAACAGGTACCAAA TCATCCATAAGTGTATGTTC
Sequence-based reagent	PF-A_FloA-6xHis_SacI	This study	PCR primer	Primer for *floA-6xHis* fragment including linker+6xHis using pIMAY; ATATTGagCtcC TTGTTGGTGGTGCTGGTGAAGAAAC
Sequence-based reagent	PR-B_FloA-6xHis	This study	PCR primer	Primer for floA-6xHis fragment including linker+6xHis using pIMAY; GTGATGGTGATGGTGATGCGATCCT CTATGTTCAGGTGACTCATCATCACTTTG
Sequence-based reagent	PF-C_FloA-6xHis	This study	PCR primer	Primer for *floA-6xHis* fragment including linker+6xHis using pIMAY; CATAGAGGATCGCATCACCATCACCATC ACTAAGTCGAGAGGTGATTAAATGAGTG
Sequence-based reagent	PR-D_FloA-6xHis_KpnI	This study	PCR primer	Primer for *floA-6xHis* fragment including linker+6xHis using pIMAY; TTTTCggTAcC AATGTCAGTACGAATCGTTTTAATATC
Sequence-based reagent	PF-A_FloA-SNAP_SacI	This study	PCR primer	Primer for *floA-SNAP* fragment using pIMAY; ATATTGagCtcCTTGTTGGTGGTGCTGGTGAAGAAAC
Sequence-based reagent	PR-B_FloA-SNAP	This study	PCR primer	Primer for *floA-SNAP* fragment using pIMAY; ATTTCGCAATCTTTGTCCATATGTT CAGGTGACTCATCATCACTTTG
Sequence-based reagent	PF-SNAP	This study	PCR primer	Primer for *floA-SNAP* fragment using pIMAY; ATGGACAAAGATTGCGAAATGAAACG
Sequence-based reagent	PR-SNAP	This study	PCR primer	Primer for *floA-SNAP* fragment using pIMAY; TCATCCCAGACCCGGTTTACCCAG
Sequence-based reagent	PF-C_FloA-SNAP	This study	PCR primer	Primer for *floA-SNAP* fragment using pIMAY; GTAAACCGGGTCTGGGATGAGTCGAGAGGTGATTAAATGAGTG
Sequence-based reagent	PR-D_FloA-SNAP_KpnI	This study	PCR primer	Primer for *floA-SNAP* fragment using pIMAY; TTTTCggTAcCAATGTCAGTACGAATCGTTTTAATATC
Sequence-based reagent	mNeon-for (NheI, SmaI)	This study	PCR primer	Primer for *isdF-mNeongreen* construct; TTATGCTAGCTTAACCCGGGATGGCGTCGAAGG
Sequence-based reagent	mNeon-rev (AscI)	This study	PCR primer	Primer for *isdF-mNeongreen* construct; TATAGGCGCGCCTCAACCTCCTTTATAGAG
Sequence-based reagent	isdF-for (NheI)	This study	PCR primer	Primer for *isdF-mNeongreen* construct; GCTCGGCTAGCATGATGATAAAAAATAAAAAG

Appendix 1—key resources table continued on next page

Appendix 1—key resources table continued

Reagent type (species) or resource	Designation	Source or reference	Identifiers	Additional information
Sequence-based reagent	isdF-rev (SmaI)	This study	PCR primer	Primer for *isdF-mNeongreen* construct; AATATCCCGGGGATTCGATTTCGTTGAC
Sequence-based reagent	pcq11-seq2-for	This study	PCR primer	Primer for *isdF-mNeongreen* construct; GTTGACTTTATCTACAAGG
Sequence-based reagent	pcq11-seq2-rev	This study	PCR primer	Primer for *isdF-mNeongreen* construct; TCTCGAAAATAATAGAGGG
Sequence-based reagent	PF_furbox + fhuC_SacI	This study	PCR primer	Primer for cloning of fur box+*fhuC* into pRB473; AAAAGAGCTCTTAGTCAATAAGATTG
Sequence-based reagent	PR_furbox + fhuC_HindIII	This study	PCR primer	Primer for cloning of fur box+*fhuC* into pRB473; ATTAACAAGCTTAATTAAGAATAAGCTCTG
Sequence-based reagent	PF_474-RBS-IsdF_PstI	This study	PCR primer	Primer for cloning *isdF-3xFLAG* into pRB474; ATGCCTGCAGaggaggattatgttATGA TGATAAAAAATAAAAAGAAACTAC
Sequence-based reagent	PR_474-IsdF	This study	PCR primer	Primer for cloning *isdF-3xFLAG* into pRB474; CCGTCATGGTCTTTGTAGTCGAT TCGATTTCGTTGACTTTGAC
Sequence-based reagent	PF-3xFLAG	This study	PCR primer	Primer for cloning *isdF-3xFLAG* into pRB474; GACTACAAAGACCATGACGGTGATTAT
Sequence-based reagent	PR-474-3xFLAG_SacI	This study	PCR primer	Primer for cloning *isdF-3xFLAG* into pRB474; TCTATgagctcTCATTTGTCATCGTCATCCTTg
Sequence-based reagent	PF_FhuB_pKT25_PstI	This study	PCR primer	Primer for cloning *fhuB* into pKT25; AAAACTGCAGTTAACATGACAAATA
Sequence-based reagent	PR_FhuB_pKT25_EcoRI	This study	PCR primer	Primer for cloning *fhuB* into pKT25; TGCGTGAATTCTTTGAACTAATCATAT
Sequence-based reagent	PF_isdF_pKT25_PstI	This study	PCR primer	Primer for cloning *isdF* into pKT25; GGATAAAAAATCTGCAGTTGATATGATGATA
Sequence-based reagent	PR_isdF-pKT25_EcoRI	This study	PCR primer	Primer for cloning *isdF* into pKT25; CACTAAACCAGGAATTCTACCGTTTTAGAT
Sequence-based reagent	MntB_KT-PF_PstI	This study	PCR primer	Primer for cloning *mntB* into pKT25; TAGTCAAAGGCTGCAGATAACATGTTAG
Sequence-based reagent	MntB_PR_EcoRI	This study	PCR primer	Primer for cloning *mntB* into pKT25; CTAATAATAAAGGTACTgAaTTcTcCATG
Sequence-based reagent	PF_pKT_SmaI	This study	PCR primer	Primer for cloning *mntB* into pKT25; GAAAACCCGGGCGTTACCCAACTTAATC

Appendix 1—key resources table continued on next page

Appendix 1—key resources table continued

Reagent type (species) or resource	Designation	Source or reference	Identifiers	Additional information
Sequence-based reagent	PR_pKT_stop_SmaI	This study	PCR primer	Primer for cloning *mntB* into pKT25; CCAGCCCGGGCGTTGTAAAACTACGG
Sequence-based reagent	PF_IsdF_short_after MCS_KpnI	This study	PCR primer	Primer for cloning *isdF_short1/2/3/4* into pKT25; GTAGGGTACCGCCGTAGTTTTACAAC
Sequence-based reagent	PR_IsdF_short_1_KpnI	This study	PCR primer	Primer for cloning *isdF_short1* into pKT25; TTGAggTaccCAAATTAAGTAAATTAG
Sequence-based reagent	PR_IsdF_short_2_KpnI	This study	PCR primer	Primer for cloning *isdF_short2* into pKT25; GTAAggtaCCCCAACTAGCTTTCTAAC
Sequence-based reagent	PR_IsdF_short_3_KpnI	This study	PCR primer	Primer for cloning *isdF_short3* into pKT25; TAGTAAAggtAccTTAGGGGACAATAG
Sequence-based reagent	PR_IsdF_short_4_KpnI	This study	PCR primer	Primer for cloning *isdF_short4* into pKT25; AGAAgGtacCAATATAATTATTAAAAATGG
Sequence-based reagent	PF_KT-IsdF_A213F	This study	PCR primer	Primer for cloning *isdF_A213F* into pKT25; CGACATACAAtttCGAAGTATCGGTTTTA ATATTGATCGTTACAGATGG
Sequence-based reagent	PR_KT-IsdF_A213F	This study	PCR primer	Primer for cloning *isdF_A213F* into pKT25; CCATCTGTAACGATCAATATTAAAACC GATACTTCGaaaTTGTATGTCG
Sequence-based reagent	PF_KT-IsdF_G217F	This study	PCR primer	Primer for cloning *isdF_G217F* into pKT25; CGACATACAAGCGCGAAGTATCttTTTTA ATATTGATCGTTACAGATGG
Sequence-based reagent	PR_KT-IsdF_G217F	This study	PCR primer	Primer for cloning *isdF_G217F* into pKT25; CCATCTGTAACGATCAATATTAAAAaaG ATACTTCGCGCTTGTATGTCG
Sequence-based reagent	PF_KT-IsdF_A+G_F	This study	PCR primer	Primer for cloning *isdF_A+G_F* into pKT25; CGACATACAAtttCGAAGTATCttTTTTA ATATTGATCGTTACAGATGG
Sequence-based reagent	PR_KT-IsdF_A+G_F	This study	PCR primer	Primer for cloning *isdF_A+G_F* into pKT25; CCATCTGTAACGATCAATATTAAAAaa GATACTTCGaaaTTGTATGTCG
Sequence-based reagent	MntB_KT-P-F (PstI)	This study	PCR primer	Primer for cloning *mntB_CH*$_{isdF}$ into pKT25; TAGTCAAAGGCTGCAGATAACATGTTAG
Sequence-based reagent	PR_MntB-CHisdF	This study	PCR primer	Primer for cloning *mntB_CH*$_{isdF}$ into pKT25; ACCGATACTTCGCGCTTGTATGTCGTCT AAATTTAGTAAATTATAGAAAATAATGAT TAGAATAAGGACGATTGAACCAATCAC

Appendix 1—key resources table continued on next page

Appendix 1—key resources table continued

Reagent type (species) or resource	Designation	Source or reference	Identifiers	Additional information
Sequence-based reagent	PF_MntB-CHisdF	This study	PCR primer	Primer for cloning *mntB_CH*$_{isdF}$ into pKT25; AATTTACTAAATTTAGACGACATACAAGCG CGAAGTATCGGTACGACGTTATTACATTAC TTTGTGATGTTGTTACTCTCATTAG
Sequence-based reagent	PR_pKT_stop_SmaI	This study	PCR primer	Primer for cloning *mntB_CH*$_{isdF}$ into pKT25; CCAGCCCGGGCGTTGTAAAACTACGG
Sequence-based reagent	PF_FhuC-SalI	This study	PCR primer	Primer for cloning *fhuC* into pUT18C; AGAAAGAAGTCGACTGAAAGTAGGGAAATTATG
Sequence-based reagent	PR_FhuC_EcoRI	This study	PCR primer	Primer for cloning *fhuC* into pUT18C; TATTGAATTCCTTAATTAAGAATAAGCTCT
Commercial assay or kit	BACTH System Kit	Euromedex	Cat. No.: EUK001	
Commercial assay or kit	CelLytic MEM protein extraction Kit	Sigma	CE0050	
Chemical compound, drug	RPMI-1640 medium	Sigma	R6504-10L	
Chemical compound, drug	Bacto casamino acids	BD Biosciences	223050	
Chemical compound, drug	EDDHA	LGC Standards	TRC-E335100-10MG	
Chemical compound, drug	Zaragozic acid A trisodium salt	Santa Cruz Biotechnology	SC-302001	
Chemical compound, drug	ONPG	Sigma	N1127	
Chemical compound, drug	DDM	Roth	CN26.1	
Chemical compound, drug	Profinity IMAC Resin Ni-charged	Bio-Rad	1560135	
Other	Ferrichrome	EMC Microcollections	FCH	See Materials and methods: Growth in iron-limited medium
Other	Aerobactin	EMC Microcollections	Fe-AERO	See Materials and methods: Growth in iron-limited medium
Other	SNAP-Cell TMR-Star	New England Biolabs	S9105S	Materials and methods: Fluorescence microscopy